519

PROPOSAL TO STUDY HIGH MOMENTUM TRANSFER PHENOMENA AND SEARCH FOR NEW STATES

Abstract

We propose an experiment to study the detailed structure of high momentum transfer multiparticle systems ("jets") at the highest energies and momentum transfers accessible at Fermilab. Special attention is paid to the possibility of detecting new particle states produced in these disruptive collisions. The proposed spectrometer configuration which covers a rapidity range of 3.8 contains three large aperture multi-cell Cerenkov counters which allow unique identification of π, K and p with momentum between $\sim$10 and 40 GeV. Operation in the existing low-halo experimental area of the proton west beam line with an interaction rate of $\sim 10^7$/spill in a thin foil Tungston target permits the study of momentum transfers up to 8 GeV/c or higher when the spectrometer is triggered with a calorimeter.

Submitted by

S. Erhan, W. Lockman, T. Meyer, M. Medinnis,
J. Rohlf and P. Schlein
University of California, Los Angeles

R. Heisterberg and L. Mo
Virginia Polytechnique Institute and State University
Blacksburg, Virginia

Correspondent: P. Schlein
Telephone: (213)825-3507

I. Introduction

Existing data[1] on correlations in high momentum transfer (P_t) reactions seem to possess a coplanar two-jet structure supporting the idea that the basic mechanism involves the scattering of hard constituents.[2] The present document is a proposal to further study such processes at the highest energies and momentum transfers accessible at Fermilab. In order to run with a target interaction rate of 10^7 interactions/spill and a large aperture spectrometer, we envisage a configuration with no detectors before the magnet; thus we require a "point" interaction source and are led to propose a transmission type experiment with a thin Tungston foil target to be located in the "halo-free" proton west beam to run with $\sim 10^{10}$ particles/spill. With the quoted interaction rate of $\sim 10^7$/spill we should be able to explore the rare events with P_t of 7 or 8 GeV/c or even larger. Hitherto, these large P_t values have only been observed at Fermilab in small aperture single particle spectrometers.[3] Our proposal is to trigger on high P_t multiparticle systems (i.e., jets) on one side of the beam line and observe the system on the other side of the beam line with a very large aperture multi-particle spectrometer.

Figure 1 shows the angular acceptance of the detectors in the center of mass together with their respective rapidity ranges. On the east side of the beam is a large aperture spectrometer (20-800 mrad in the lab; a mean azimuthal range of 40°) containing three multi-cell Cerenkov counters for π, K and p identification over a large range of momenta. As shown, the rapidity range "seen" is considerably larger than the range of $\Delta y \sim 2$ observed by many experimenters,[1] and interpreted as jet correlations.

The apparatus on the west side of the beam refered to as "trigger" in Figure 1 consists of a multi-cell calorimeter with frontal area 2 x 1.5 m positioned 10 m from the target. Between target and calorimeter are three

measuring stations of multi-wire proportional chambers for momentum analysis of charged tracks useful in calibration of the calorimeter and also to detect spill-over of some tracks from objects with smaller P_t whose decay products lie on both sides of the beam.

Based on the single particle high P_t cross sections of Cronin et al[3] and our large interaction rate we can expect to see P_t values of 8 GeV/c or larger in the calorimeter. The recent results of the E260 collaboration[4] (in the M6 beam) that the single particle high P_t cross sections are only a small fraction ($\sim 10^{-2}$) of the higher multiplicity high P_t cross sections (including neutrals), as had been expected on the basis of earlier ISR results and phenomenology,[5] implies together with the results of Reference (3) that our high P_t "jet" trigger rate will be large (e.g., 20/spill at $P_t \sim 8$ GeV/c).

The rapidity ranges shown in Figure 1 for calorimeter and spectrometer are well matched. Assuming a jet rapidity range of $\Delta y \sim 2$, it is easily seen that the acceptances well accommodate not only "back-to-back" jets but also "non-collinear" jets, as expected to frequently occur (since the lab is not in general the parton-parton center of mass).

Another facet of studying the detailed structure of high P_t jets will be to search for new states as well as already known ones. It seems likely that the very disruptive nature of the collisions which produce high P_t systems may also make them abundant producers of charm and other exotic states. The apparent ineffectiveness of single lepton triggers as signatures for charm production and decay makes it all the more interesting to pursue the line suggested here.

When the high intensity pion beam becomes operational, it will be desirable to move the detectors downstream to that area. It should also be noted the experimental configuration is admirably suitable for operation

in a 1000 GeV external beam of the proton lab when it is available.

The remainder of this proposal contains the following items:

II Spectrometer Description

III Trigger Calorimeter

IV Spectrometer Acceptance of Charmed Particles

V Trigger Rates

VI Run Request and Time Scale

VII Computing

Figures 2 (a,b) show the center-of-mass to lab kinematics for 400 GeV (and 1000 GeV) incident beam for reference in the following sections. In the plane of x (in the CM) and $P_\perp$ are plotted lines of constant lab angle and lab energy. The spectrometer detects between 20 and 800 mrad. The lab energy lines delineate the various regions of Cerenkov identification as discussed below.

II. Spectrometer Description

(a) General Discussion

In an attempt to optimize geometrical acceptance, particle identification and resolution, in addition to having high rate capability, we have arrived at the design shown in Figure 3. The proton west beam vacuum pipe passes through the magnetic aperture of a large window frame magnet (the non-interacting beam experiences a bend of $\Delta\theta \sim 1$ mrad which will have to be compensated for downstream of our experiment). The beam interacts in a thin foil Tungston target inside the vacuum pipe. The final-state particles emerge from the thin-walled vacuum pipe and are detected by the principle spectrometer on the east side of the beam pipe. This detector system consists of three multi-cell Cerenkov counters, the first of which is inserted in the magnet, four large area two-dimensional readout drift chambers and a multi-wire proportional chamber. The laboratory angular acceptance of this system is $20 < \theta < 800$ mradian, thus allowing the spectrometer to cover the major part of the center-of-mass.

On the west side of the beam pipe is a large trigger calorimeter positioned 10 m from the target with laboratory angular acceptance $10 < \theta < 210$ mrad and an array of multi-wire proportional chamgers. The increased density of MWPC near the calorimeter is to permit a long decay path for K^o and Λ^o and subsequent measurement of their decay tracks.

(b) Magnet

The magnet is an Argonne type SCM105 with pole pieces 84" wide by 30" deep and a field of 18 kGauss with a gap of 14". (The gap may be enlarged to 30" if we desire). The field integral with the 14" gap is $\sim$13.5 kGauss-meter corresponding to a momentum transfer kick of 0.4 GeV/c.

In discussions with Russ Clem at Argonne we have learned that prospects for using one of these magnets in the very near future are quite favorable. The power requirements are ∿3/4 Megawatt. The exterior dimensions of the magnet at beam elevation are ∿200" wide by ∿50" deep, much too large to fit through the access port to the proton west area. Thus, either the magnet must be disassembled or the access port must be substantially enlarged.

(c) Target and Beam-Line Vacuum Chamber

According to Cox and Murphy[6] the present spot size at the center of the target hall in proton west is 4.5 mm horizontally by 0.5 mm vertically, which is ideal for our application. However, since our target will be positioned at the upstream end of the target hall at the entrance to the pretarget tunnel, where they quote the beam sizes to be 10 mm horizontally by 6 mm vertically, it seems likely that the last set of quadrupole magnets will have to be moved upstream somewhat in the tunnel in order to reduce the beam size at our proposed target position.

The target will consist of a thin Tungsten foil with thickness transverse to the beam (∿0.2 mm) and length along the beam (∿1 mm), compatible with resolution of the spectrometer. The vertical source size is given by the beam spot size (0.5 mm). This target yields 10^7 interactions/spill with a beam of $\sim 10^{10}$/spill. The vacuum pipe after the target position should be 0.15 mm thick cylindrical stainless steel with a surface corregation similar to that used in several ISR experiments to minimize interactions of particles exiting the vacuum pipe.

Figure 4 shows the probable layout of the target, vacuum pipe, C_1 and first set of chambers which allows for the emergence of small angle particles with minimum interaction. 60 mrad particles emerge from

the vacuum pipe early enough to enter the first Cerenkov counter. Particles with $30 < \theta < 60$ mrad emerge through the corregation. Between 10 and 20 mrad, they traverse the 1 mm thick end piece. Thus, for the worst case of 30 mrad, with the corrugation depth (6 mm) and spacing (25 mm), the exiting particle traverses 200 mm of the corrugated section or 200/25 x 2 = 16 wall thicknesses = 2.4 mm of steel. We have assumed a diameter of 6 cm for the corregated pipe in Figure 4. This is somewhat smaller than the 15 cm usually used at the ISR but should present no particular problem in fabrication.

(d) Cerenkov counters

The three Cerenkov counters shown in Figure 3 are filled with gases at atmospheric pressure to yield unambiguous π, κ and p identification from 12-40 GeV. This latter situation is achieved with Freon 22; air and 90% helium, respectively. With neopentane in C_1, for example, efficient pion separation from kaons and protons starts at $\sim$3 GeV,but full π, κ, p separation is obtained only between 8-16 and $\sim$20-40 GeV. The lines of constant lab energy in Figures 2(a,b) allow the reader to see the X-P_t area in the center-of-mass covered by the Cerenkov counters.

C_1 is a 6-cell counter inserted in the magnet and is similar to such counters constructed by some of us for use in a recent ISR experiment.[7] A radiation length of $\sim$1.5 meters with RCA 8854 5" tubes will yield $\sim$8-10 photoelectrons for β=1 particles.

C_2 (22 cells) and C_3 (16 cells) are the UCLA counters presently in use at the MPS. E260 has just ended and E110 is scheduled to run in February 1977. Afterwards, the counters can be removed and modified for the proton-west experiment proposed here.

(e) Two Dimensional Readout Drift Chambers

These chambers positioned before and after C_2 in Figure 3 contain delay lines ($\sim$100 nsec/25 cm) adjacent to the sense wire and therefore yield for each track traversing a chamber a course (y) coordinate with σ_y = 3 mm in addition to the precision x-coordinate, for which we hope to achieve $\sigma_x \sim 0.2$ mm. A small test chamber has already been constructed and successfully tested in a beam.[7] See Figure 5 for the results. At the present time two larger chambers are under construction by us with dimensions 0.6 x 1.7 m. These will serve as prototypes for the chambers needed here. It may be noted that the use of these two-dimensional chambers simplifies pattern recognition problems and thus reduces computer usage. Two layers of chambers will be used bfore C_2 (separated by 0.5 m) and two layers after C_2 (also separated by 0.5 m). Straight lines can thus be found in these chambers with an accuracy of better than 0.1 mrad.

(f) Multi-Wire Proportional Chambers

These chambers (12 planes) exist[8] and are presently in use by some of us in the muon lab. After the completion of E369 next spring, they could be moved to proton-west for use in this experiment. They are 1 m x 1 m and have a wire spacing of 1.5 mm.

One plane with horizontal wires will be positioned just in front of C_2 for use in improving the y-coordinate precision. Nine planes will be used on the west side of the beam line in front of the calorimeter to measure the charged trigger particles as well as some decay products of those states which yield products on both sides of the beam line. They will aid in calorimeter calibration and in addition, will also permit the reconstruction of Λ^o and K^o decays, for which knowledge of the momenta of the decay tracks is not essential. A decay length of $\sim$8 meters is available for this purpose.

(g) Hodoscope

This large hodoscope positioned after C_3, whose signals will be time-digitized with each event, will serve to provide a more precise time coincidence statement for each track reconstructed from the chamber information, thus allowing accidental background tracks to be removed.

III. Trigger Calorimeter

The calorimeter shown in Figure 3 is 1.5 m high and 2.0 m wide. Its depth in iron along the beam is to be 1.0 m or ∿6 interaction lengths. The iron will consist of fifty 1.5 m x 2.0 m sheets each 2 cm thick, sandwiched between sheets of 6 mm thick (1/4") plastic scintillator. The scintillator will consist of 20 cm wide x 1.5 m high vertical strips. One photomultiplier on top and one on the bottom will read out each 10 scintillator strips. These photomultiplier signals will be linearly added to give one signal. Thus, a total of 10 (transversely) x 5 (in depth) = 50 signals will be added together (after weighting each according to the θ_{Lab} angle of its cell) to give the total P_t signal.

Having a total of five longitudinal sections for each angular cell will allow us to weight unusually high energy deposition, such as result from electromagnetic conversion of some of the energy, if additional energy resolution is necessary.[9] Also, energy loss out the back of the calorimeter can be corrected for, if necessary, by adding additional counters at the rear of the calorimeter. We plan to at least reach the resolution obtained by Engler et al.[10] They found $\sigma = \pm 9\%$ for $E = 25$ GeV. We should be able to obtain $\sigma \approx \pm 6$ or 7% at $E = 100$ GeV. This improved calorimeter resolution, in addition to the higher energy that corresponds to a given P_t, at 400 GeV as compared, say, to 200 GeV, should make a marked improvement in triggering efficiency over previous experiments.

IV. Spectrometer Acceptance of Charm Particles

Figures 6-8 show constant percentage acceptance contours of the apparatus for the following objects produced at different x-P_t values

$$pp \rightarrow D^{\pm}_{0} + X$$
$$\hookrightarrow K^{+}\pi^{-}$$
$$\hookrightarrow K^{+}\pi^{+}\pi^{-}$$
$$\hookrightarrow K^{+}\pi^{-}\pi^{+}\pi^{-}$$

both for the observed mass of the state (1.87 GeV) and also for a ficticious higher mass state at 3 GeV. The calculations assume phase space decay of the D.

The acceptance is seen to be quite good.

V. Trigger Rates and Background

The high P_t trigger rates can be estimated from the 400 GeV results of Cronin et al.[3] Shown in Figure 9 are the expected number of triggers per spill, per GeV in P_t. The quoted Cronin et al single nucleon cross sections for π's, K's and p's of both charges are multiplied by a factor of 40 to give the total single particle high P_t cross section on Tungston. With our calorimeter dimensions discussed in Section III, we estimate the total jet cross section in the calorimeter to be $\sim$100 times larger than the single particle cross section. (The jet trigger is obtained by adding together the pulse heights in all cells (weighted by angle) before discrimination.) We obtain this number from the corresponding enhancement factor of 50 to 100 quoted by the E260 collaboration[4] and take the larger value because one calorimeter with twice the area is more efficient at accepting the entire jet with a rapidity range $\Delta y \sim 2$.

There are two additional relevant factors in these trigger considerations. One is the effect that the calorimeter energy resolution has on causing more frequent lower P_t signals to satisfy the trigger. The other factor is the background triggers caused by halo particles. With the calorimeter specifications given in Section III, we expect to have a resolution of $\sigma \sim 6\%$ or so when $P_t \sim$ 7-8 GeV/c (at 90^o in the center-of-mass). This results in a P_t spread of $\sim \pm 1$ GeV/c at these large P_t values. In other words, with a trigger threshold set at, say, 7 GeV/c, we will have a comparable contribution from $\sim$6 GeV/c as from 7 GeV/c.

As for halo considerations, we quote Cox and Murphy[6] who claim a halo rate of $\sim 150/10^{10}$ beam/cm^2 at 5.6 cm from the center line. These rates are observed to decrease exponentially out to 40 cm from center line. Singles rates are perhaps 10x larger but are of no concern to us because our calorimeter trigger will be in coincidence with the large counter hodoscope

on the other side of the beam line. Thus, we anticipate no particular difficulties in achieving the trigger rates given in Figure 9. We expect that these rates may be uncertain to a factor of 2 or 4. Even if they were a factor of 10x too large, the effectiveness of the experiment would not be appreciably damaged.

VI. Run Request and Time Scale

We request a total of 900 hours for this experiment; 300 for testing and debugging, and 600 for data taking.

We estimate that the first large drift chamber could be installed not later than April or May 1977 and the remaining ones by July 1977. The calorimeter should also be ready by April or May 1977. Target tests with several proportional chambers and the smaller drift chambers presently being constructed could be carried out as early as March 1977.

VII. Computing

We remark that the UCLA group's Eclipse computer (1/3 the computing power of the 6600) will be completely dedicated to the analysis of this experiment.

References

1. See, e.g., the recent rapporteur talk by P. Darriulat at the XVIII International Conference on High Energy Physics, Tblisi, USSR (1976). See also P. Darriulat, Nucl. Physics. B107, 429 (1976).

2. See, e.g., the rapporteur talk by P. V. Landshoff in Proceedings of the XVII International Conference on High Energy Physics, London (1974), page V-57.

3. J. W. Cronin et al, Phys. Rev. Letters 31, 1426 (1973).

4. Caltech-UCLA-Chicago Circle-FNAL-Indiana E260 collaboration to be presented at APS topical conference on High Energy Physics, BNL (10/6/76).

5. S. D. Ellis, M. Jacob and P. V. Landshoff, Jets and Correlations in Large P_T Reactions, TH.2109-CERN (12/18/75).

6. B. Cox and C. T. Murphy, The Design and Performance of a Halo-Free Intense Extracted Proton Beam at Fermilab, Nucl. Inst. and Methods (in press, 1976).

7. M. Atac, R. Bosshard, S. Erhan and P. Schlein, A Two-Dimensional Drift Chamber, Nucl. Inst. and Methods (in press, 1976).

8. K. B. Burns, B. R. Grummon, T. A. Nunamaker, L. W. Mo and S. C. Wright, Nucl. Inst. and Methods 106, 171 (1973).

9. H. Hilscher et al, Proceedings of the Calorimeter Workshop, FNAL (May 1975), page 295.

10. J. Engler et al, Nucl. Inst. and Methods 106, 189 (1973).

Figure Captions

(1) Acceptance angular regions in the center-of-mass for the spectrometer on the east side of beam line and trigger calorimeter on the west side of beam line. The center-of-mass rapidity ranges of each are also shown.

(2) Kinematic curves relating center-of-mass variables and laboratory variables (energy and angle) for beam momenta: (a) 400 GeV/c and (b) 1000 GeV/c.

(3) Layout of apparatus in P-west area. D_1-D_4 are two-dimensional readout drift chambers, S_1 and S_2 are hodoscopes. The target position is shown with an X near the entrance to the room.

(4) Details of target region and first $\sim$2.5 m of the beam vacuum pipe. C_1 is the first Cerenkov counter. The corregation has a depth of 6 mm and a period of 25 mm.

(5) Typical difference of delay line coordinate measurements and beam track MWPC measurements (wire spacing in MWPC 1 mm).

(6-8) Contours in the center-of-mass X-P_t plane of constant percentage acceptance of $K\pi$, $K\pi\pi$ and $K\pi\pi\pi$ systems with invariant masses 1.87 and 3.0 GeV. Curves were calculated with a Monte Carlo program. Systems are assumed to decay with phase-space distributions.

(9) Estimated number of jet triggers per unit interval of P_t per spill, estimated as described in the text.

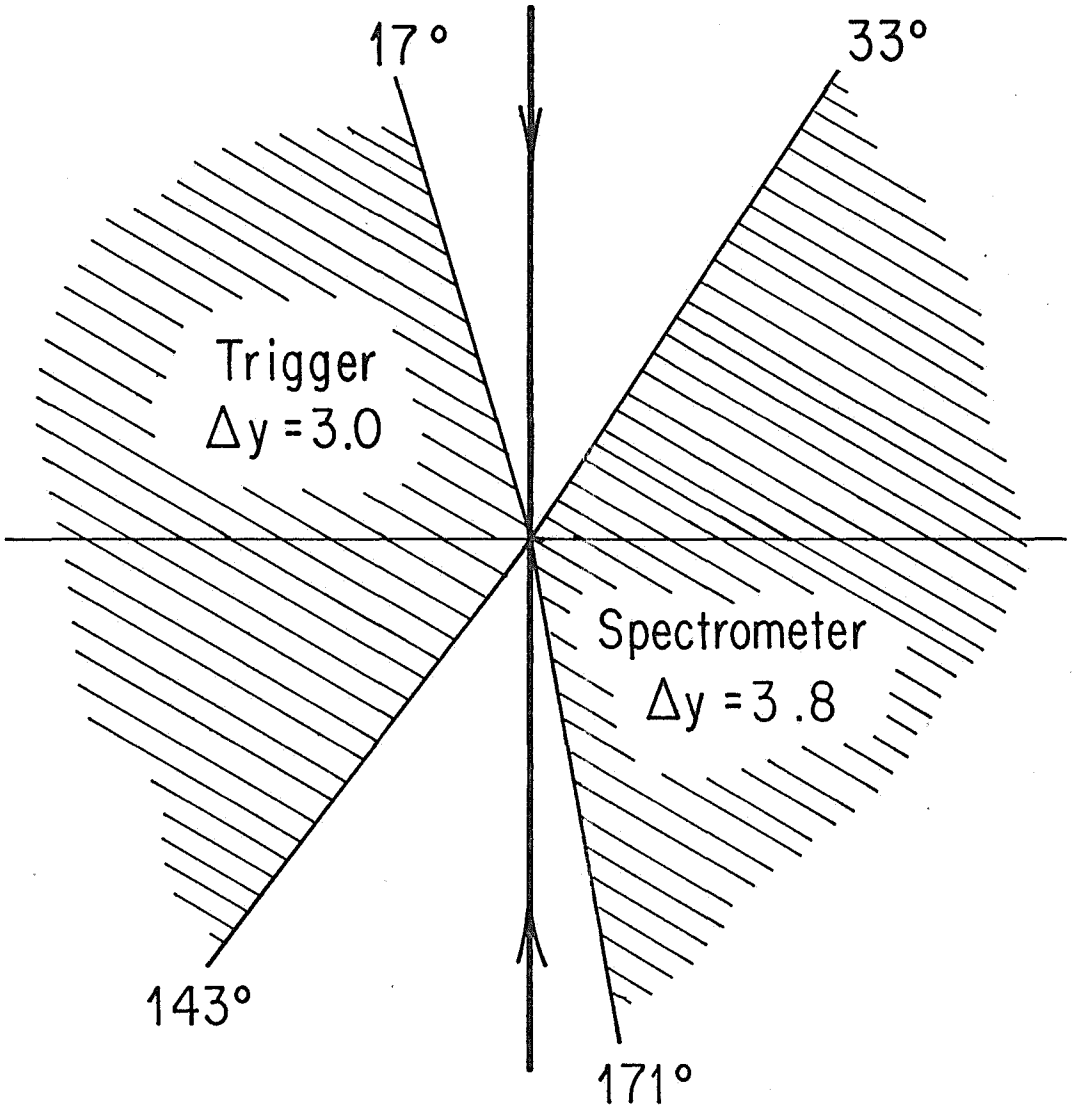
C.M. Angles (400 GeV)
17°
33°
Trigger
Δy = 3.0
Spectrometer
Δy = 3.8
143°
171°

FIG. 1

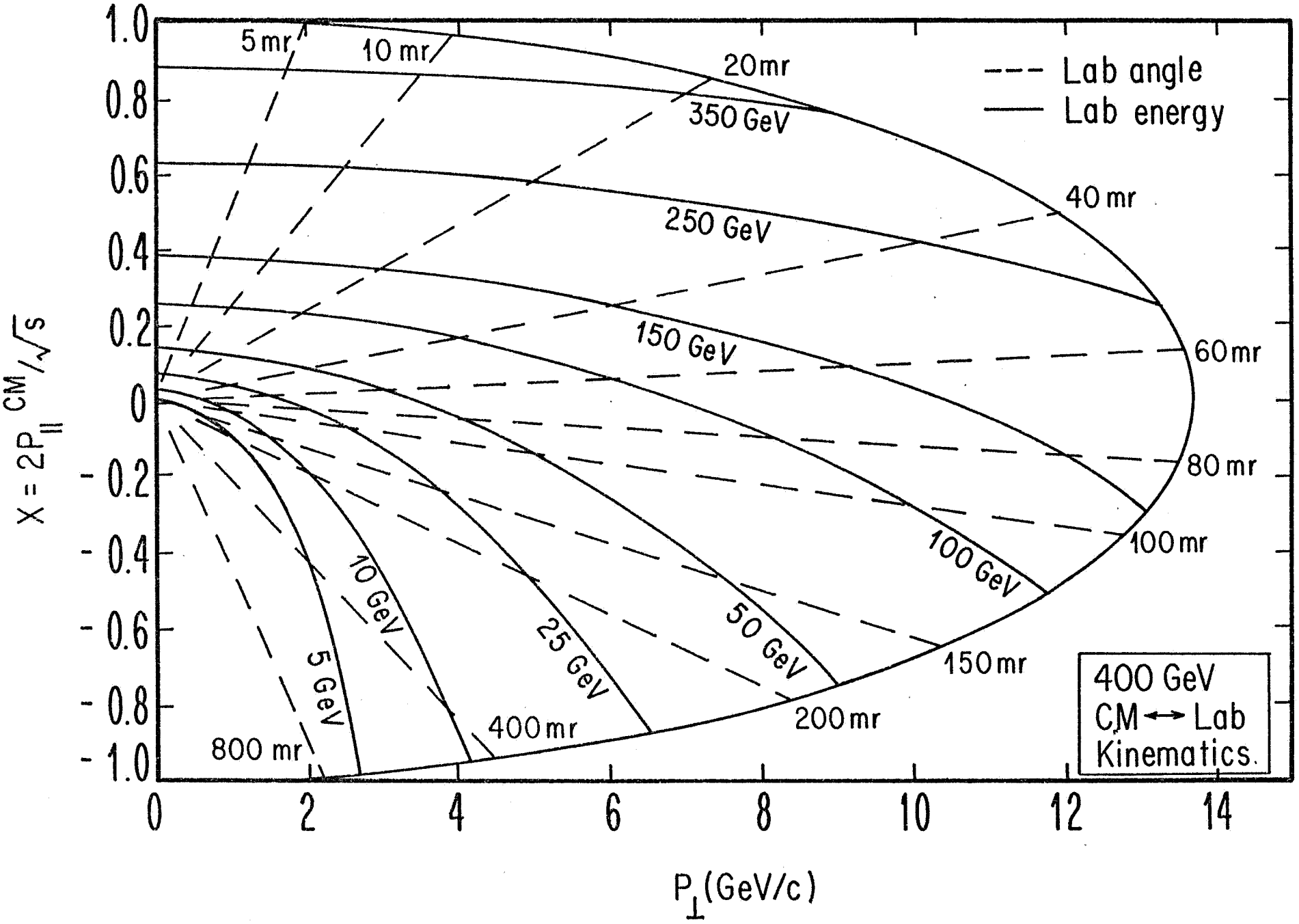
Lab angle
Lab energy
5 mr
10 mr
20 mr
40 mr
60 mr
80 mr
100 mr
150 mr
200 mr
400 mr
800 mr
350 GeV
250 GeV
150 GeV
100 GeV
50 GeV
25 GeV
10 GeV
5 GeV
400 GeV
CM ↔ Lab
Kinematics.
$X = 2P_{\parallel}^{CM}/\sqrt{s}$
$P_{\perp}$ (GeV/c)
1.0
0.8
0.6
0.4
0.2
0
- 0.2
- 0.4
- 0.6
- 0.8
- 1.0
0
2
4
6
8
10
12
14

Fig 29

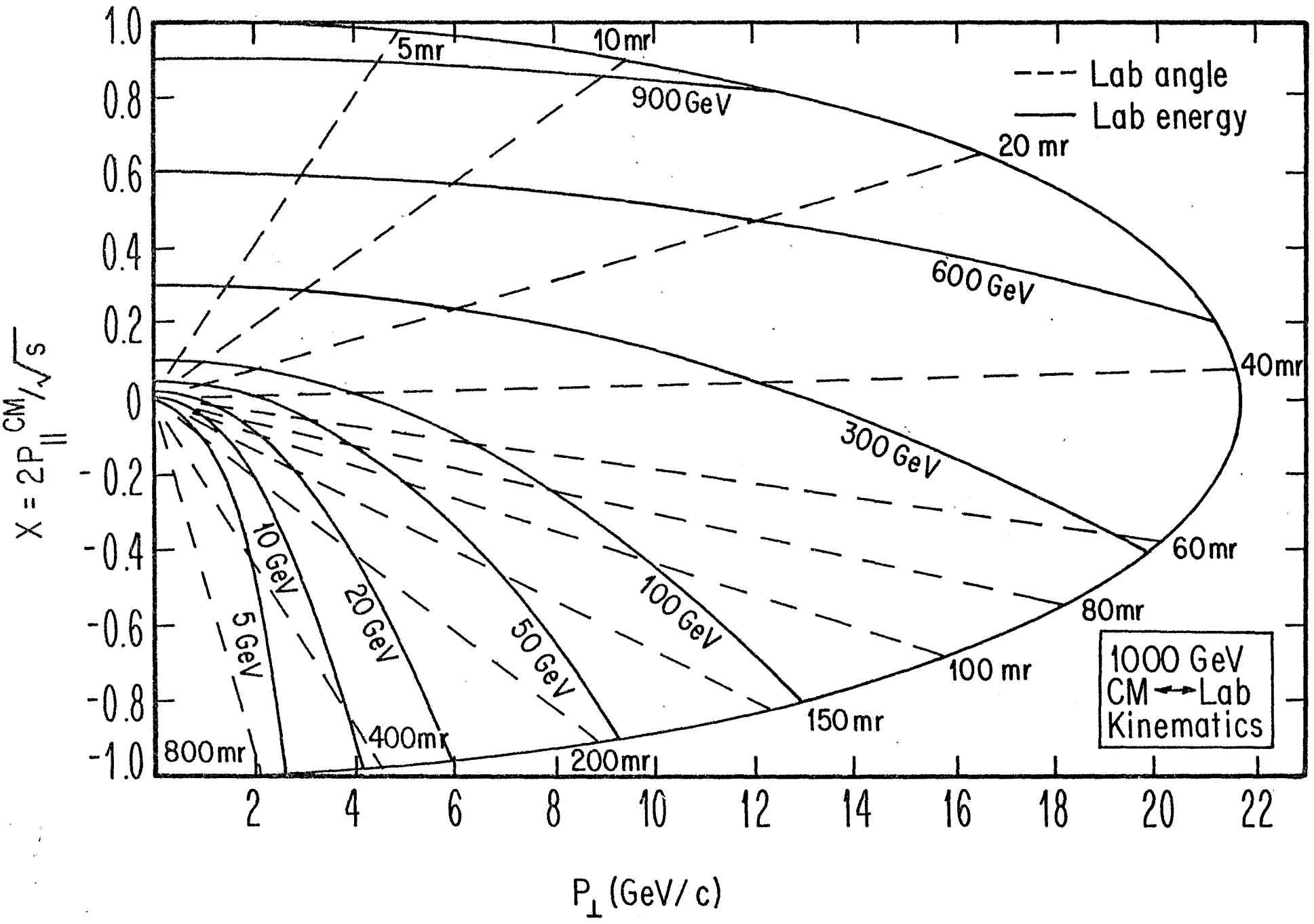
Lab angle
Lab energy
1000 GeV
CM ↔ Lab
Kinematics
5mr
10mr
20 mr
40mr
60mr
80mr
100 mr
150 mr
200mr
400mr
800mr
900 GeV
600 GeV
300 GeV
100 GeV
50 GeV
20 GeV
10 GeV
5 GeV
$X = 2P_{\parallel}^{CM}/\sqrt{s}$
$P_{\perp}$ (GeV/c)

Fig-26

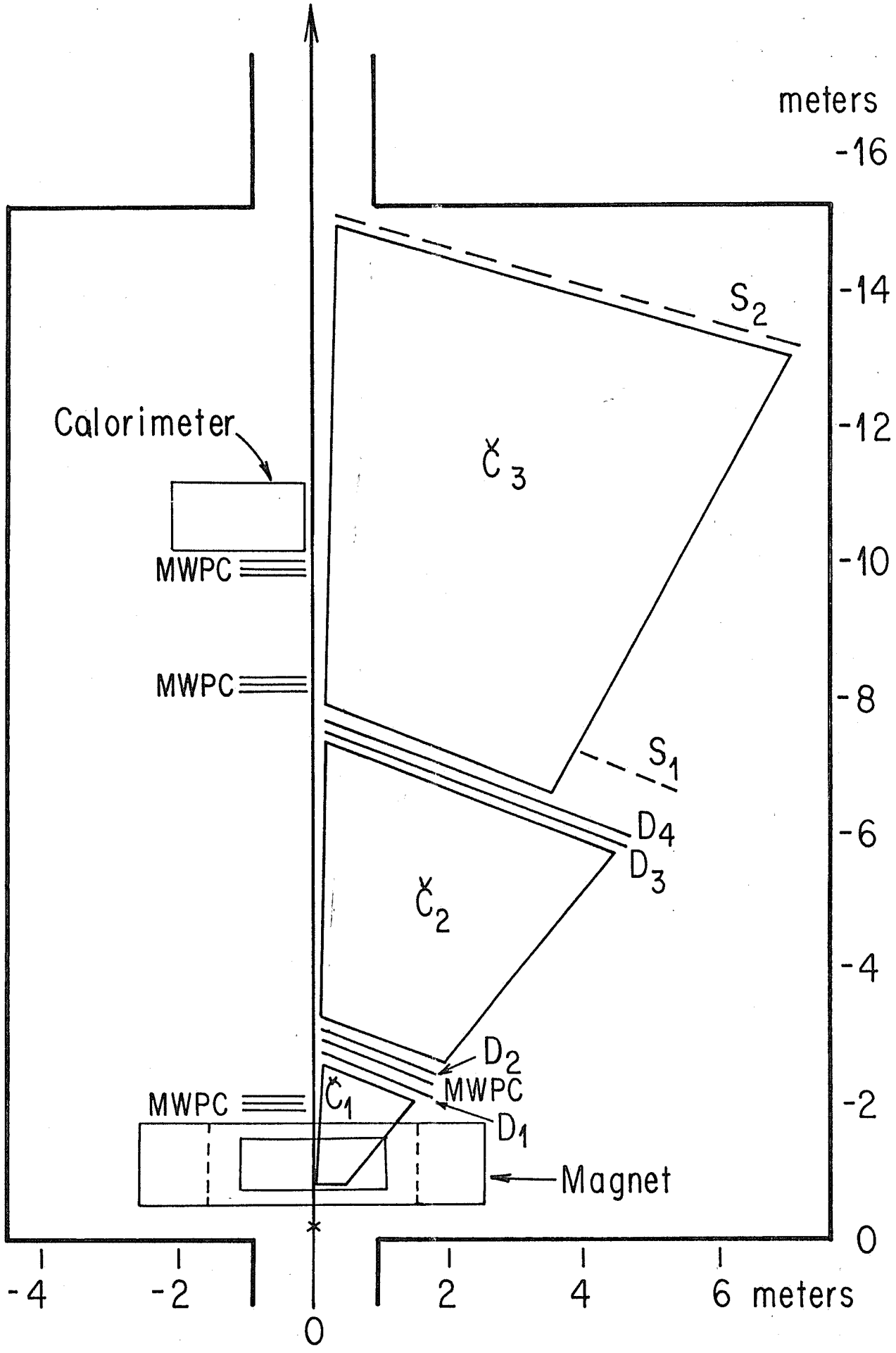
meters
-16
-14
-12
-10
-8
-6
-4
-2
0
S2
Calorimeter
C̆3
MWPC
MWPC
S1
D4
D3
C̆2
D2
MWPC
MWPC
C̆1
D1
Magnet
-4
-2
0
2
4
6 meters

FIG 3

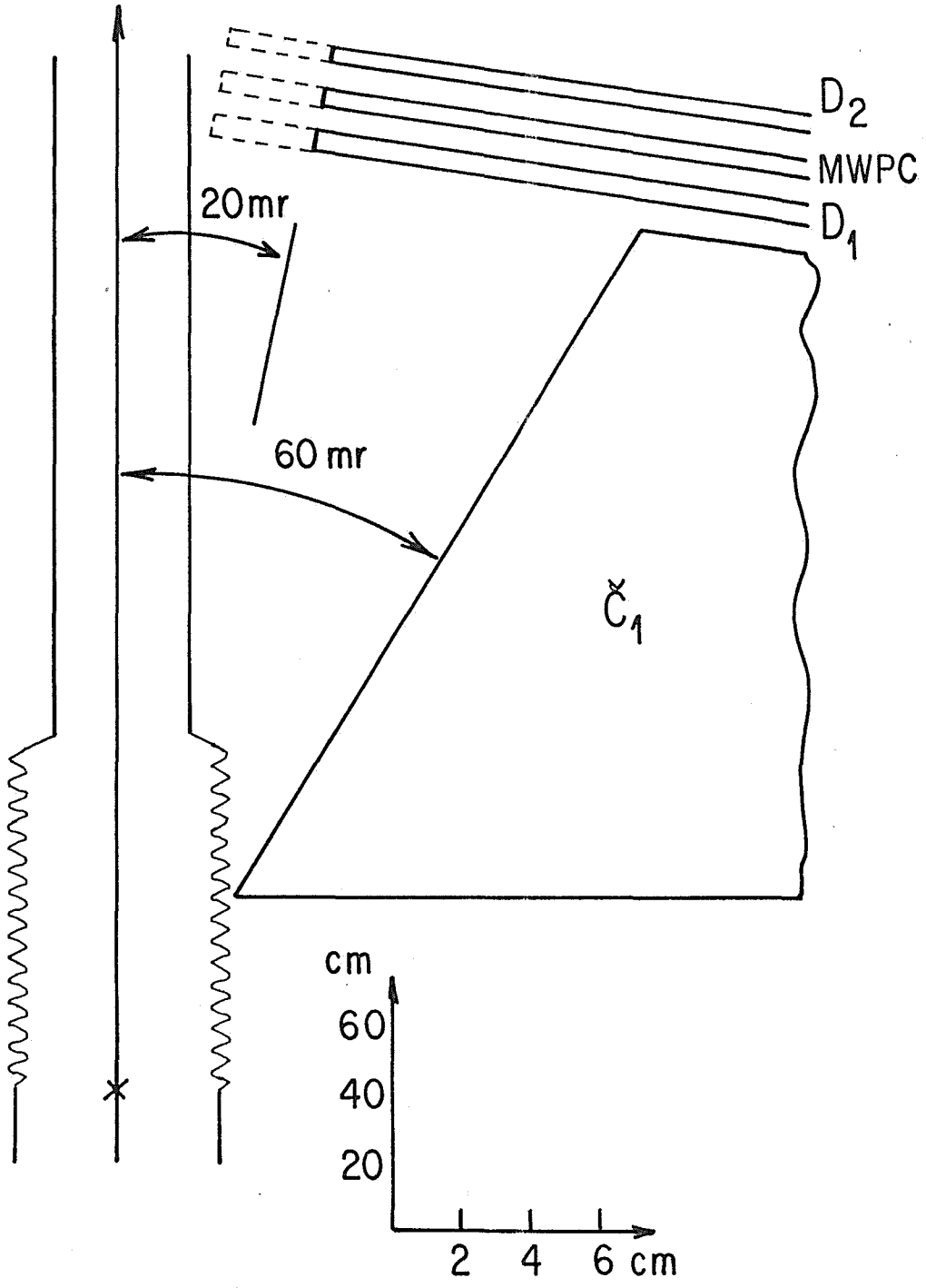

FIG 4

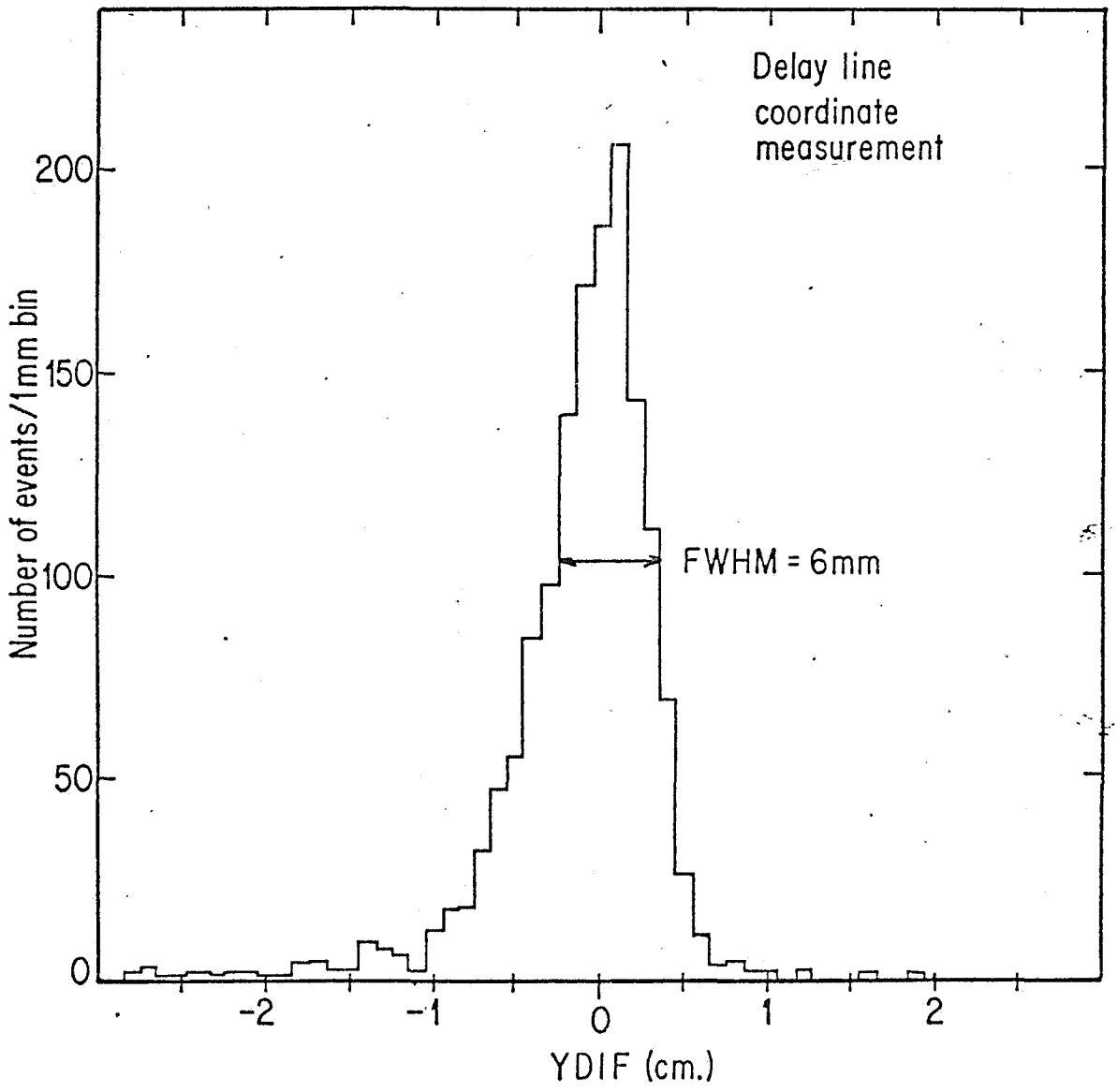
Delay line
coordinate
measurement
FWHM = 6mm
Number of events/1mm bin
200
150
100
50
0
-2
-1
0
1
2
YDIF (cm.)

FIG. 5

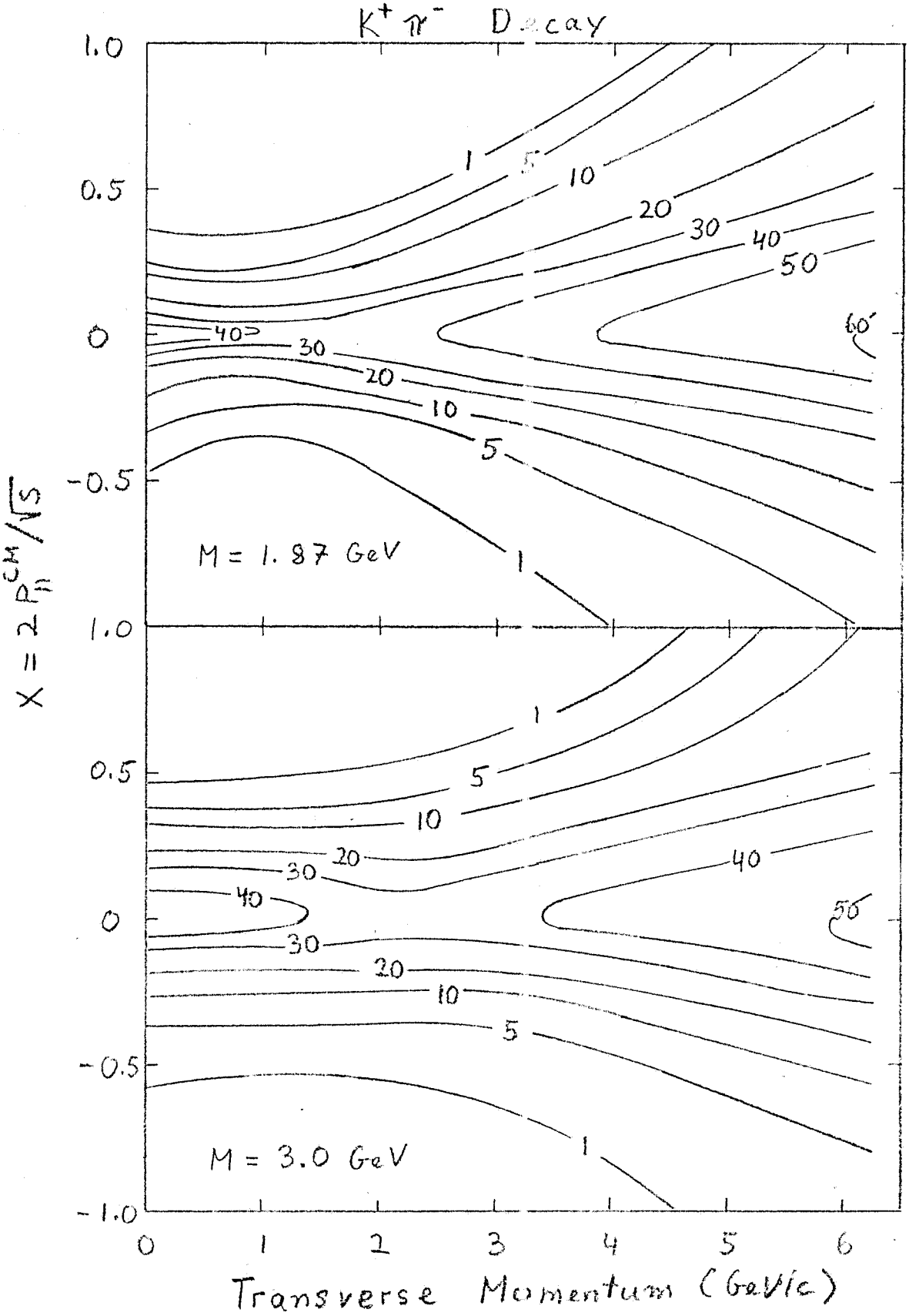
$K^+\pi^-$ Decay
1.0
0.5
0
-0.5
1.0
0.5
0
-0.5
-1.0
0
1
2
3
4
5
6
1
5
10
20
30
40
50
60
40
30
20
10
5
1
M = 1.87 GeV
1
5
10
20
30
40
50
40
30
20
10
5
1
M = 3.0 GeV
$X = 2P_{\parallel}^{CM}/\sqrt{s}$
Transverse Momentum (GeV/c)

FIG. 6

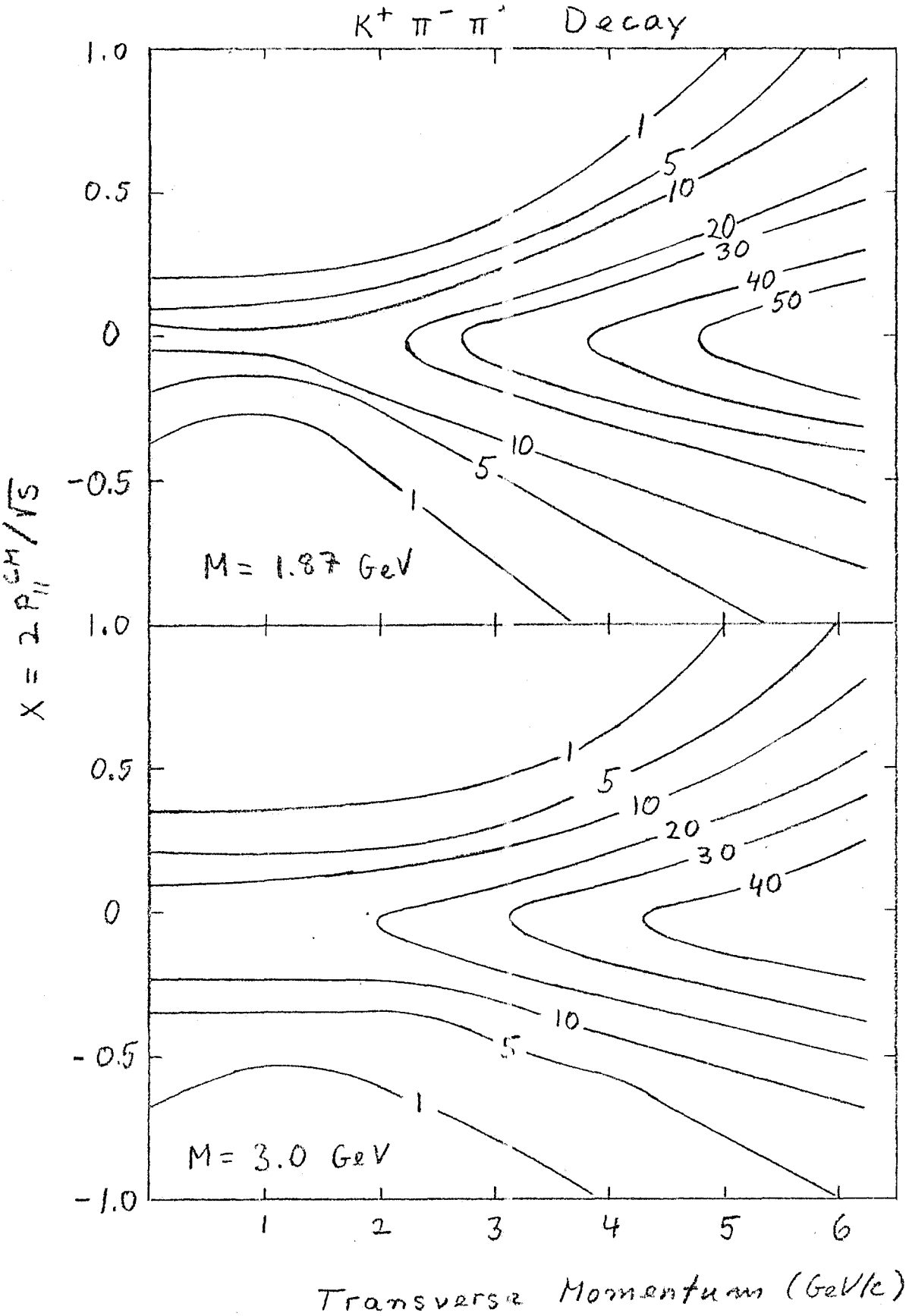
$K^+ \pi^- \pi^-$ Decay
1.0
0.5
0
-0.5
1.0
0.5
0
-0.5
-1.0
1
5
10
20
30
40
50
10
5
1
M = 1.87 GeV
1
5
10
20
30
40
10
5
1
M = 3.0 GeV
1
2
3
4
5
6
$X = 2P_{\parallel}^{CM}/\sqrt{s}$
Transverse Momentum (GeV/c)

FIG. 7

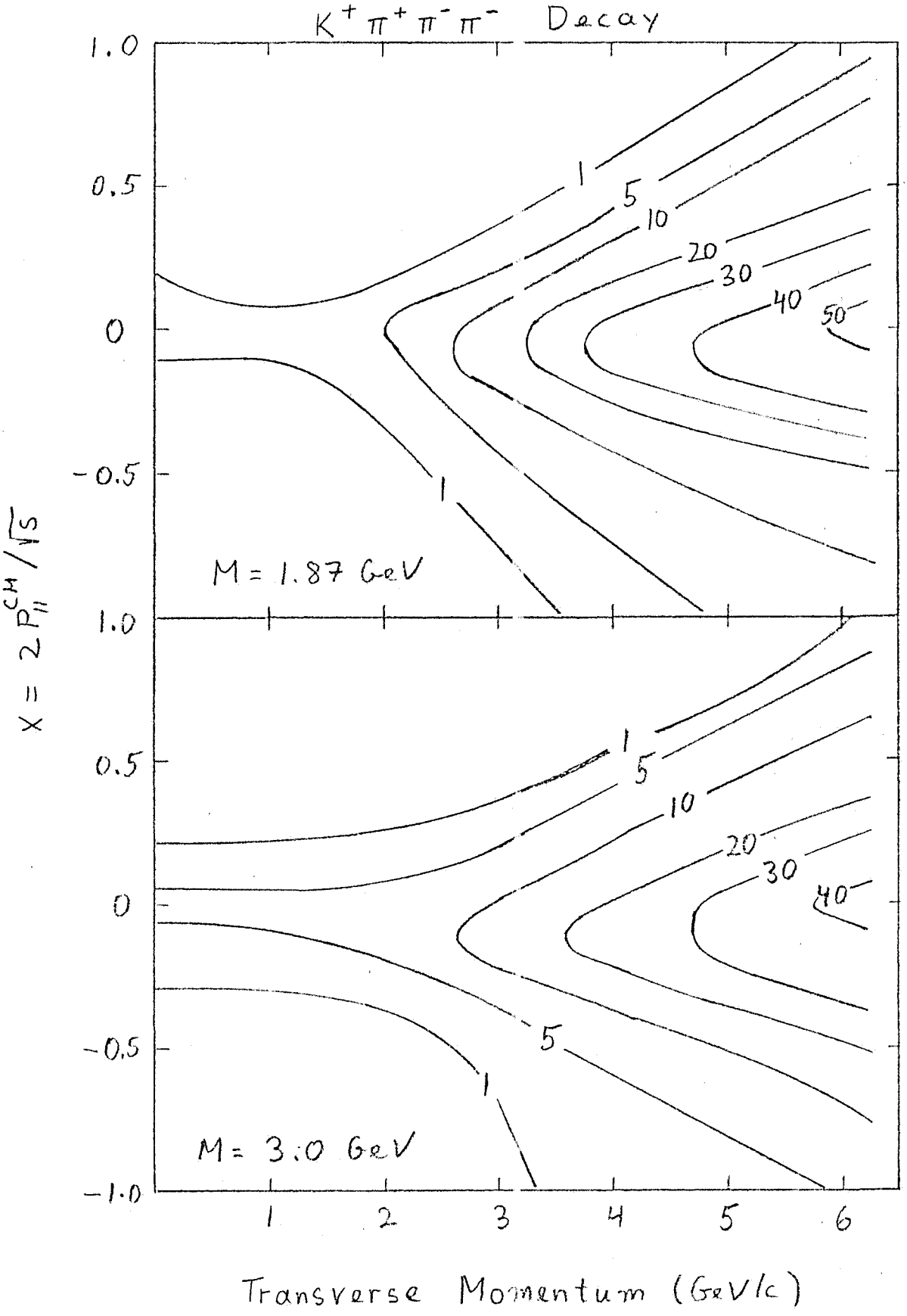
$K^+\pi^+\pi^-\pi^-$ Decay
1.0
0.5
0
-0.5
1.0
0.5
0
-0.5
-1.0
1
5
10
20
30
40
50
1
5
10
20
30
40
1
5
1
M = 1.87 GeV
M = 3.0 GeV
$X = 2P_{11}^{CM}/\sqrt{s}$
1
2
3
4
5
6
Transverse Momentum (GeV/c)

FIG 8

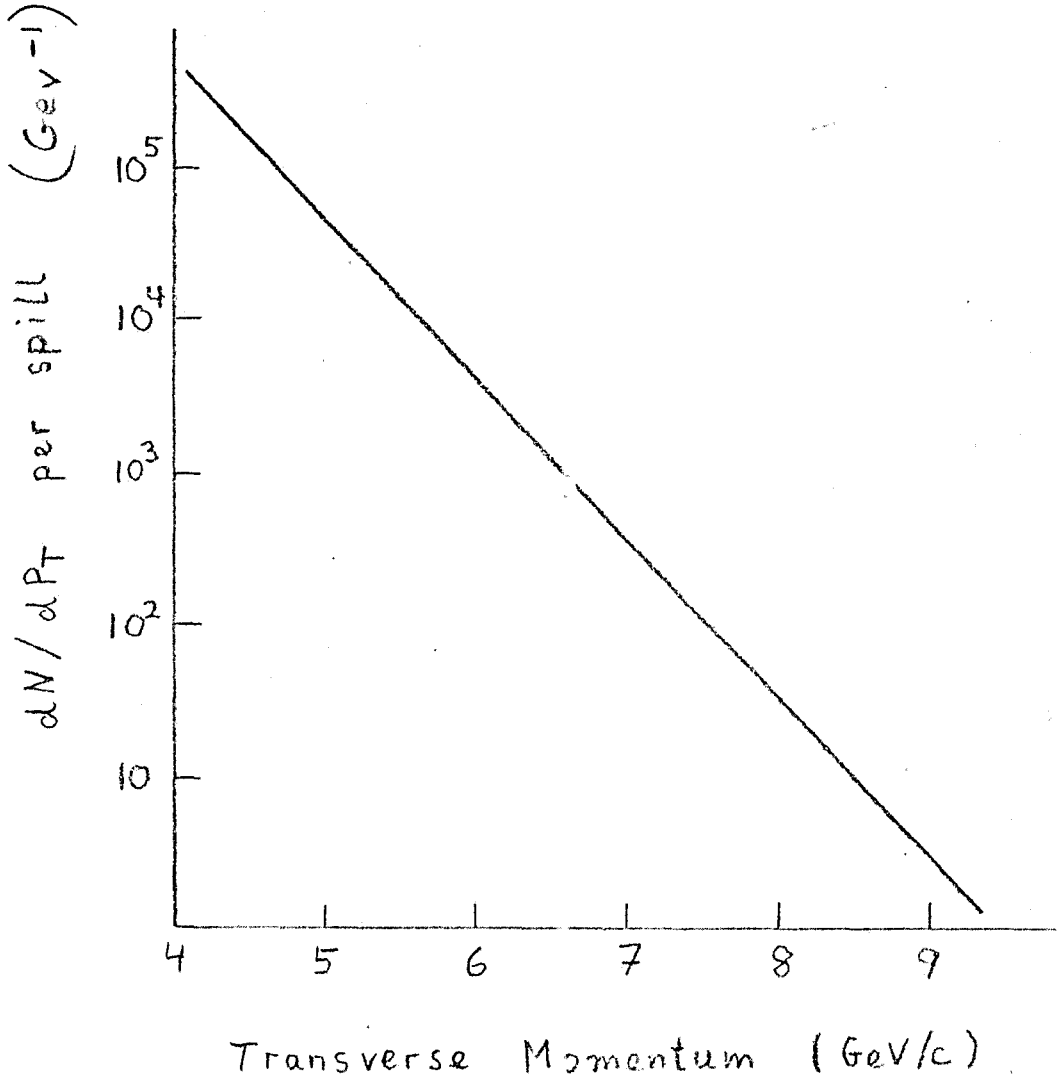
dN/dP_T per spill (Gev^-1)
10^5
10^4
10^3
10^2
10
4
5
6
7
8
9
Transverse Momentum (GeV/c)

FIG. 9

//Revised//

PROPOSAL TO STUDY HIGH MOMENTUM TRANSFER PHENOMENA AND SEARCH FOR NEW STATES

Abstract

We propose an experiment to study the detailed structure of high momentum transfer multiparticle systems ("jets") at the highest energies and momentum transfers accessible at Fermilab. Special attention is paid to the possibility of detecting new particle states produced in these disruptive collisions. The proposed spectrometer configuration which covers a rapidity range of 3.8 contains three large aperture multi-cell Cerenkov counters which allow unique identification of π, κ and p with momentum between $\sim$10 and 40 GeV. Operation in the existing low-halo experimental area of the proton west beam line with an interaction rate of $\sim 10^7$/spill in a thin foil Tungston target permits the study of momentum transfers up to 8 GeV/c or higher when the spectrometer is triggered with a calorimeter.

Submitted by

S. Erhan, W. Lockman, T. Meyer, M. Medinnis,
J. Rohlf and P. Schlein
University of California, Los Angeles

R. Heisterberg and L. Mo
Virginia Polytechnique Institute and State University
Blacksburg, Virginia

October 1, 1976

Correspondent: P. Schlein
Telephone: (213)825-3507

I. Introduction

Existing data[1] on correlations in high momentum transfer (P_t) reactions seem to possess a coplanar two-jet structure supporting the idea that the basic mechanism involves the scattering of hard constituents.[2] The present document is a proposal to further study such processes at the highest energies and momentum transfers accessible at Fermilab. In order to run with a target interaction rate of 10^7 interactions/spill and a large aperture spectrometer, we envisage a configuration with no detectors before the magnet; thus we require a "point" interaction source and are led to propose a transmission type experiment with a thin Tungston foil target to be located in the "halo-free" proton west beam to run with $\sim 10^{10}$ particles/spill. With the quoted interaction rate of $\sim 10^7$/spill we should be able to explore the rare events with P_t of 7 or 8 GeV/c or even larger. Hitherto, these large P_t values have only been observed at Fermilab in small aperture single particle spectrometers.[3] Our proposal is to trigger on high P_t multiparticle systems (i.e., jets) on one side of the beam line and observe the system on the other side of the beam line with a very large aperture multi-particle spectrometer.

Figure 1 shows the angular acceptance of the detectors in the center of mass together with their respective rapidity ranges. On the east side of the beam is a large aperture spectrometer (20-800 mrad in the lab; a mean azimuthal range of 40^o) containing three multi-cell Cerenkov counters for π, κ and p identification over a large range of momenta. As shown, the rapidity range "seen" is considerably larger than the range of $\Delta y \sim 2$ observed by many experimenters,[1] and interpreted as jet correlations.

The apparatus on the west side of the beam refered to as "trigger" in Figure 1 consists of a multi-cell calorimeter with frontal area 2 x 1.5 m positioned 10 m from the target. Between target and calorimeter are three

measuring stations of multi-wire proportional chambers for momentum analysis of charged tracks useful in calibration of the calorimeter and also to detect spill-over of some tracks from objects with smaller P_t whose decay products lie on both sides of the beam.

Based on the single particle high P_t cross sections of Cronin et al[3] and our large interaction rate we can expect to see P_t values of 8 GeV/c or larger in the calorimeter. The recent results of the E260 collaboration[4] (in the M6 beam) that the single particle high P_t cross sections are only a small fraction ($\sim 10^{-2}$) of the higher multiplicity high P_t cross sections (including neutrals), as had been expected on the basis of earlier ISR results and phenomenology,[5] implies together with the results of Reference (3) that our high P_t "jet" trigger rate will be large (e.g., $\sim$1/spill at $P_t \sim 8$ GeV/c).

The rapidity ranges shown in Figure 1 for calorimeter and spectrometer are well matched. Assuming a jet rapidity range of $\Delta y \sim 2$, it is easily seen that the acceptances well accommodate not only "back-to-back" jets but also "non-collinear" jets, as expected to frequently occur (since the lab is not in general the parton-parton center of mass).

Another facet of studying the detailed structure of high P_t jets will be to search for new states as well as already known ones. It seems likely that the very disruptive nature of the collisions which produce high P_t systems may also make them abundant producers of charm and other exotic states. The apparent ineffectiveness of single lepton triggers as signatures for charm production and decay makes it all the more interesting to pursue the line suggested here.

When the high intensity pion beam becomes operational, it will be desirable to move the detectors downstream to that area. It should also be noted the experimental configuration is admirably suitable for operation

in a 1000 GeV external beam of the proton lab when it is available.

The remainder of this proposal contains the following items:

II Spectrometer Description

III Trigger Calorimeter

IV Spectrometer Acceptance of Charmed Particles

V Trigger Rates

VI Run Request and Time Scale

VII Computing

Figures 2 (a,b) show the center-of-mass to lab kinematics for 400 GeV (and 1000 GeV) incident beam for reference in the following sections. In the plane of x (in the CM) and $P_\perp$ are plotted lines of constant lab angle and lab energy. The spectrometer detects between 20 and 800 mrad. The lab energy lines delineate the various regions of Cerenkov identification as discussed below.

II. Spectrometer Description

(a) General Discussion

In an attempt to optimize geometrical acceptance, particle identification and resolution, in addition to having high rate capability, we have arrived at the design shown in Figure 3. The proton west beam vacuum pipe passes through the magnetic aperture of a large window frame magnet (the non-interacting beam experiences a bend of $\Delta\theta \sim 1$ mrad which will have to be compensated for downstream of our experiment). The beam interacts in a thin foil Tungston target inside the vacuum pipe. The final-state particles emerge from the thin-walled vacuum pipe and are detected by the principle spectrometer on the east side of the beam pipe. This detector system consists of three multi-cell Cerenkov counters, the first of which is inserted in the magnet, four large area two-dimensional readout drift chambers and a multi-wire proportional chamber. The laboratory angular acceptance of this system is $20 < \theta < 800$ mradian, thus allowing the spectrometer to cover the major part of the center-of-mass.

On the west side of the beam pipe is a large trigger calorimeter positioned 10 m from the target with laboratory angular acceptance $10 < \theta < 210$ mrad and an array of multi-wire proportional chamgers. The increased density of MWPC near the calorimeter is to permit a long decay path for K^o and Λ^o and subsequent measurement of their decay tracks.

(b) Magnet

The magnet is an Argonne type SCM105 with pole pieces 84" wide by 30" deep and a field of 18 kGauss with a gap of 14". (The gap may be enlarged to 30" if we desire). The field integral with the 14" gap is $\sim$13.5 kGauss-meter corresponding to a momentum transfer kick of 0.4 GeV/c.

In discussions with Russ Clem at Argonne we have learned that prospects for using one of these magnets in the very near future are quite favorable. The power requirements are ∿3/4 Megawatt. The exterior dimensions of the magnet at beam elevation are ∿200" wide by ∿50" deep, much too large to fit through the access port to the proton west area. Thus, either the magnet must be disassembled or the access port must be substantially enlarged.

(c) Target and Beam-Line Vacuum Chamber

According to Cox and Murphy[6] the present spot size at the center of the target hall in proton west is 4.5 mm horizontally by 0.5 mm vertically, which is ideal for our application. However, since our target will be positioned at the upstream end of the target hall at the entrance to the pretarget tunnel, where they quote the beam sizes to be 10 mm horizontally by 6 mm vertically, it seems likely that the last set of quadrupole magnets will have to be moved upstream somewhat in the tunnel in order to reduce the beam size at our proposed target position.

The target will consist of a thin Tungsten foil with thickness transverse to the beam (∿0.2 mm) and length along the beam (∿1 mm), compatible with resolution of the spectrometer. The vertical source size is given by the beam spot size (0.5 mm). This target yields 10^7 interactions/spill with a beam of $\sim 10^{10}$/spill. The vacuum pipe after the target position should be 0.15 mm thick cylindrical stainless steel with a surface corregation similar to that used in several ISR experiments to minimize interactions of particles exiting the vacuum pipe.

Figure 4 shows the probable layout of the target, vacuum pipe, C_1 and first set of chambers which allows for the emergence of small angle particles with minimum interaction. 60 mrad particles emerge from

the vacuum pipe early enough to enter the first Cerenkov counter. Particles with $30 < \theta < 60$ mrad emerge through the corregation. Between 20 and 30 mrad, they traverse the 1 mm thick end piece. Thus, for the worst case of 30 mrad, with the corrugation depth (6 mm) and spacing (25 mm), the exiting particle traverses 200 mm of the corrugated section or 200/25 x 2 = 16 wall thicknesses = 2.4 mm of steel. We have assumed a diameter of 6 cm for the corregated pipe in Figure 4. This is somewhat smaller than the 15 cm usually used at the ISR but should present no particular problem in fabrication.

(d) Cerenkov counters

The three Cerenkov counters shown in Figure 3 are filled with gases at atmospheric pressure to yield unambiguous π, κ and p identification from 12-40 GeV. This latter situation is achieved with Freon 22; air and 90% helium, respectively. With neopentane in C_1, for example, efficient pion separation from kaons and protons starts at $\sim$3 GeV,but full π, κ, p separation is obtained only between 8-16 and $\sim$20-40 GeV. The lines of constant lab energy in Figures 2(a,b) allow the reader to see the X-P_t area in the center-of-mass covered by the Cerenkov counters.

C_1 is a 6-cell counter inserted in the magnet and is similar to such counters constructed by some of us for use in a recent ISR experiment. A radiation length of $\sim$1.5 meters with RCA 8854 5" tubes will yield $\sim$8-10 photoelectrons for β=1 particles.

C_2 (22 cells) and C_3 (16 cells) are the UCLA counters presently in use at the MPS. E260 has just ended and E110 is scheduled to run in February 1977. Afterwards, the counters can be removed and modified for the proton-west experiment proposed here.

(e) Two Dimensional Readout Drift Chambers

These chambers positioned before and after C_2 in Figure 3 contain delay lines (∿100 nsec/25 cm) adjacent to the sense wire and therefore yield for each track traversing a chamber a course (y) coordinate with σ_y = 3 mm in addition to the precision x-coordinate, for which we hope to achieve $\sigma_x \sim 0.2$ mm. A small test chamber has already been constructed and successfully tested in a beam.[7] See Figure 5 for the results. At the present time two larger chambers are under construction by us with dimensions 0.6 x 1.7 m. These will serve as prototypes for the chambers needed here. It may be noted that the use of these two-dimensional chambers simplifies pattern recognition problems and thus reduces computer usage. Two layers of chambers will be used bfore C_2 (separated by 0.5 m) and two layers after C_2 (also separated by 0.5 m). Straight lines can thus be found in these chambers with an accuracy of better than 0.1 mrad.

(f) Multi-Wire Proportional Chambers

These chambers (12 planes) exist[8] and are presently in use by some of us in the muon lab. After the completion of E369 next spring, they could be moved to proton-west for use in this experiment. They are 1 m x 1 m and have a wire spacing of 1.5 mm.

One plane with horizontal wires will be positioned just in front of C_2 for use in improving the y-coordinate precision. Nine planes will be used on the west side of the beam line in front of the calorimeter to measure the charged trigger particles as well as some decay products of those states which yield products on both sides of the beam line. They will aid in calorimeter calibration and in addition, will also permit the reconstruction of Λ^o and K^o decays, for which knowledge of the momenta of the decay tracks is not essential. A decay length of ∿8 meters is available for this purpose.

(g) Hodoscope

This large hodoscope positioned after C_3, whose signals will be time-digitized with each event, will serve to provide a more precise time coincidence statement for each track reconstructed from the chamber information, thus allowing accidental background tracks to be removed.

III. Trigger Calorimeter

The calorimeter shown in Figure 3 is 1.5 m high and 2.0 m wide. Its depth in iron along the beam is to be 1.0 m or ∿6 interaction lengths. The iron will consist of fifty 1.5 m x 2.0 m sheets each 2 cm thick, sandwiched between sheets of 6 mm thick (1/4") plastic scintillator. The scintillator will consist of 20 cm wide x 1.5 m high vertical strips. One photomultiplier on top and one on the bottom will read out each 10 scintillator strips. These photomultiplier signals will be linearly added to give one signal. Thus, a total of 10 (transversely) x 5 (in depth) = 50 signals will be added together (after weighting each according to the θ_{Lab} angle of its cell) to give the total P_t signal.

Having a total of five longitudinal sections for each angular cell will allow us to weight unusually high energy deposition, such as result from electromagnetic conversion of some of the energy, if additional energy resolution is necessary.[9] Also, energy loss out the back of the calorimeter can be corrected for, if necessary, by adding additional counters at the rear of the calorimeter. We plan to at least reach the resolution obtained by Engler et al.[10] They found $\sigma = \pm 9\%$ for $E = 25$ GeV. We should be able to obtain $\sigma \approx \pm 6$ or 7% at $E = 100$ GeV. This improved calorimeter resolution, in addition to the higher energy that corresponds to a given P_t at 400 GeV as compared, say, to 200 GeV should make a marked improvement in triggering efficiency over previous experiments.

A similar array of lead-scintillator sandwich 15-20 radiation lengths thick will be positioned in front of the hadron calorimeter to measure the neutral energy.

IV. Spectrometer Acceptance of Charm Particles

Figures 6-8 show constant percentage acceptance contours of the apparatus for the following objects produced at different x-P_t values

$$pp \to \overset{+}{D^0} + X$$
$$\hookrightarrow K^+\pi^-$$
$$\hookrightarrow K^+\pi^+\pi^-$$
$$\hookrightarrow K^+\pi^-\pi^+\pi^-$$

both for the observed mass of the state (1.87 GeV) and also for a ficticious higher mass state at 3 GeV. The calculations assume phase space decay of the D.

The acceptance is seen to be quite good.

V. Trigger Rates and Background

The high P_t trigger rates can be estimated from the 400 GeV results of Cronin et al.[3] Shown in Figure 9 are the expected number of triggers per spill, per GeV in P_t. The quoted Cronin et al single nucleon cross sections for π's, K's and p's of both charges are multiplied by a factor of 40 to give the total single particle high P_t cross section on Tungsten. With our calorimeter dimensions discussed in Section III, we estimate the total jet cross section in the calorimeter to be $\sim$100 times larger than the single particle cross section. (The jet trigger is obtained by adding together the pulse heights in all cells (weighted by angle) before discrimination.) We obtain this number from the corresponding enhancement factor of 50 to 100 quoted by the E260 collaboration[4] and take the larger value because one calorimeter with twice the area is more efficient at accepting the entire jet with a rapidity range $\Delta y \sim 2$.

There are two additional relevant factors in these trigger considerations. One is the effect that the calorimeter energy resolution has on causing more frequent lower P_t signals to satisfy the trigger. The other factor is the background triggers caused by halo particles. With the calorimeter specifications given in Section III, we expect to have a resolution of $\sigma \sim 6\%$ or so when $P_t \sim$ 7-8 GeV/c (at 90° in the center-of-mass). This results in a P_t spread of $\sim \pm 1$ GeV/c at these large P_t values. In other words, with a trigger threshold set at, say, 7 GeV/c, we will have a comparable contribution from $\sim$6 GeV/c as from 7 GeV/c.

As for halo considerations, we quote Cox and Murphy[6] who claim a halo rate of $\sim 150/10^{10}$ beam/cm^2 at 5.6 cm from the center line. These rates are observed to decrease exponentially out to 40 cm from center line. Singles rates are perhaps 10x larger but are of no concern to us because our calorimeter trigger will be in coincidence with the large counter hodoscope

on the other side of the beam line. Thus, we anticipate no particular difficulties in achieving the trigger rates given in Figure 9. We expect that these rates may be uncertain to a factor of 2 or 4. Even if they were a factor of 10x too large, the effectiveness of the experiment would not be appreciably damaged.

VI. Run Request and Time Scale

We request a total of 900 hours for this experiment; 300 for testing and debugging, and 600 for data taking.

We estimate that the first large drift chamber could be installed not later than April or May 1977 and the remaining ones by July 1977. The calorimeter should also be ready by April or May 1977. Target tests with several proportional chambers and the smaller drift chambers presently being constructed could be carried out as early as March 1977.

VII. Computing

We remark that the UCLA group's Eclipse computer (1/3 the computing power of the 6600) will be completely dedicated to the analysis of this experiment.

References

1. See, e.g., the recent rapporteur talk by P. Darriulat at the XVIII International Conference on High Energy Physics, Tblisi, USSR (1976). See also P. Darriulat, Nucl. Physics. B107, 429 (1976).

2. See, e.g., the rapporteur talk by P. V. Landshoff in Proceedings of the XVII International Conference on High Energy Physics, London (1974), page V-57.

3. J. W. Cronin et al, Phys. Rev. Letters 31, 1426 (1973).

4. Caltech-UCLA-Chicago Circle-FNAL-Indiana E260 collaboration to be presented at APS topical conference on High Energy Physics, BNL (10/6/76).

5. S. D. Ellis, M. Jacob and P. V. Landshoff, Jets and Correlations in Large P_T Reactions, TH.2109-CERN (12/18/75).

6. B. Cox and C. T. Murphy, The Design and Performance of a Halo-Free Intense Extracted Proton Beam at Fermilab, Nucl. Inst. and Methods (in press, 1976).

7. M. Atac, R. Bosshard, S. Erhan and P. Schlein, A Two-Dimensional Drift Chamber, Nucl. Inst. and Methods (in press, 1976).

8. K. B. Burns, B. R. Grummon, T. A. Nunamaker, L. W. Mo and S. C. Wright, Nucl. Inst. and Methods 106, 171 (1973).

9. H. Hilscher et al, Proceedings of the Calorimeter Workshop, FNAL (May 1975), page 295.

10. J. Engler et al, Nucl. Inst. and Methods 106, 189 (1973).

Figure Captions

(1) Acceptance angular regions in the center-of-mass for the spectrometer on the east side of beam line and trigger calorimeter on the west side of beam line. The center-of-mass rapidity ranges of each are also shown.

(2) Kinematic curves relating center-of-mass variables and laboratory variables (energy and angle) for beam momenta: (a) 400 GeV/c and (b) 1000 GeV/c.

(3) Layout of apparatus in P-west area. D_1-D_4 are two-dimensional readout drift chambers, S_1 and S_2 are hodoscopes. The target position is shown with an X near the entrance to the room.

(4) Details of target region and first $\sim$2.5 m of the beam vacuum pipe. $\check{C}_1$ is the first Cerenkov counter. The corregation has a depth of 6 mm and a period of 25 mm.

(5) Typical difference of delay line coordinate measurements and beam track MWPC measurements (wire spacing in MWPC 1 mm).

(6-8) Contours in the center-of-mass X-P_t plane of constant percentage acceptance of $K\pi$, $K\pi\pi$ and $K\pi\pi\pi$ systems with invariant masses 1.87 and 3.0 GeV. Curves were calculated with a Monte Carlo program. Systems are assumed to decay with phase-space distributions.

(9) Estimated number of jet triggers per unit interval of P_t per spill, estimated as described in the text.

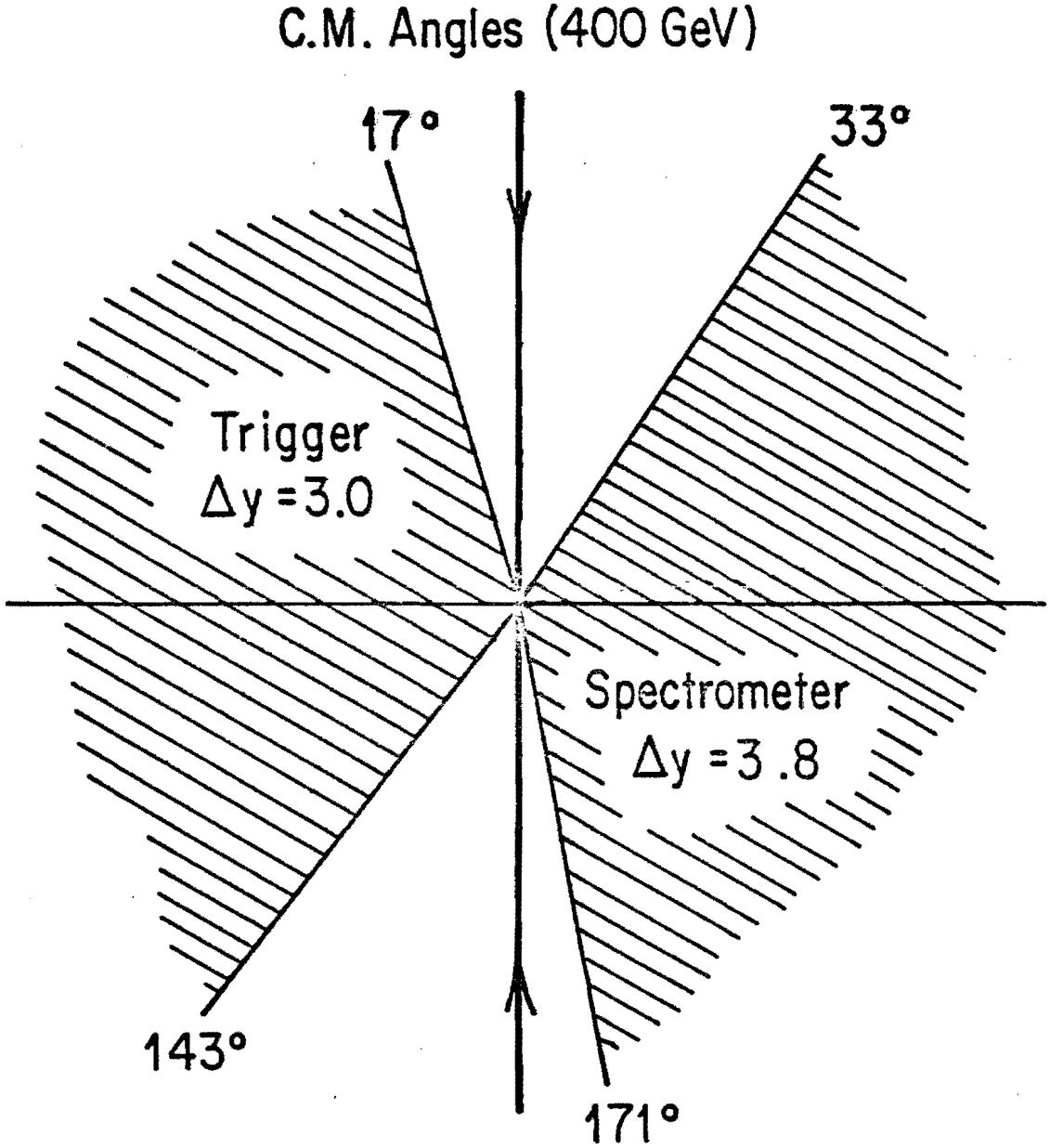
C.M. Angles (400 GeV)
17°
33°
Trigger
Δy = 3.0
Spectrometer
Δy = 3.8
143°
171°

FIG. 1

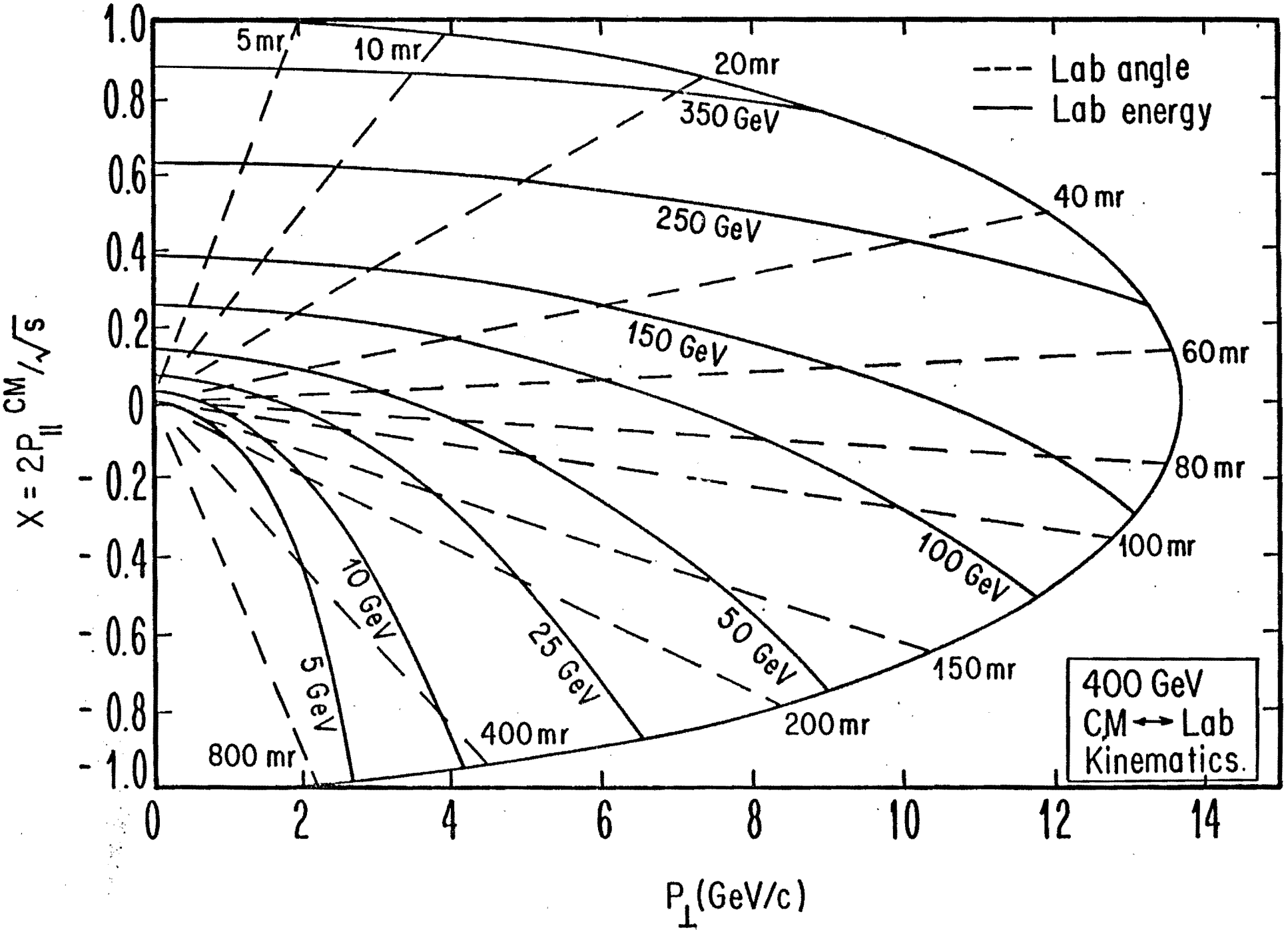
1.0
0.8
0.6
0.4
0.2
0
- 0.2
- 0.4
- 0.6
- 0.8
- 1.0
$X = 2P_{\parallel}^{CM}/\sqrt{s}$
0
2
4
6
8
10
12
14
$P_\perp$ (GeV/c)
5 mr
10 mr
20mr
40 mr
60mr
80 mr
100mr
150mr
200mr
400mr
800 mr
350 GeV
250 GeV
150 GeV
100 GeV
50 GeV
25 GeV
10 GeV
5 GeV
--- Lab angle
—— Lab energy
400 GeV
CM ↔ Lab
Kinematics.

Fig 29

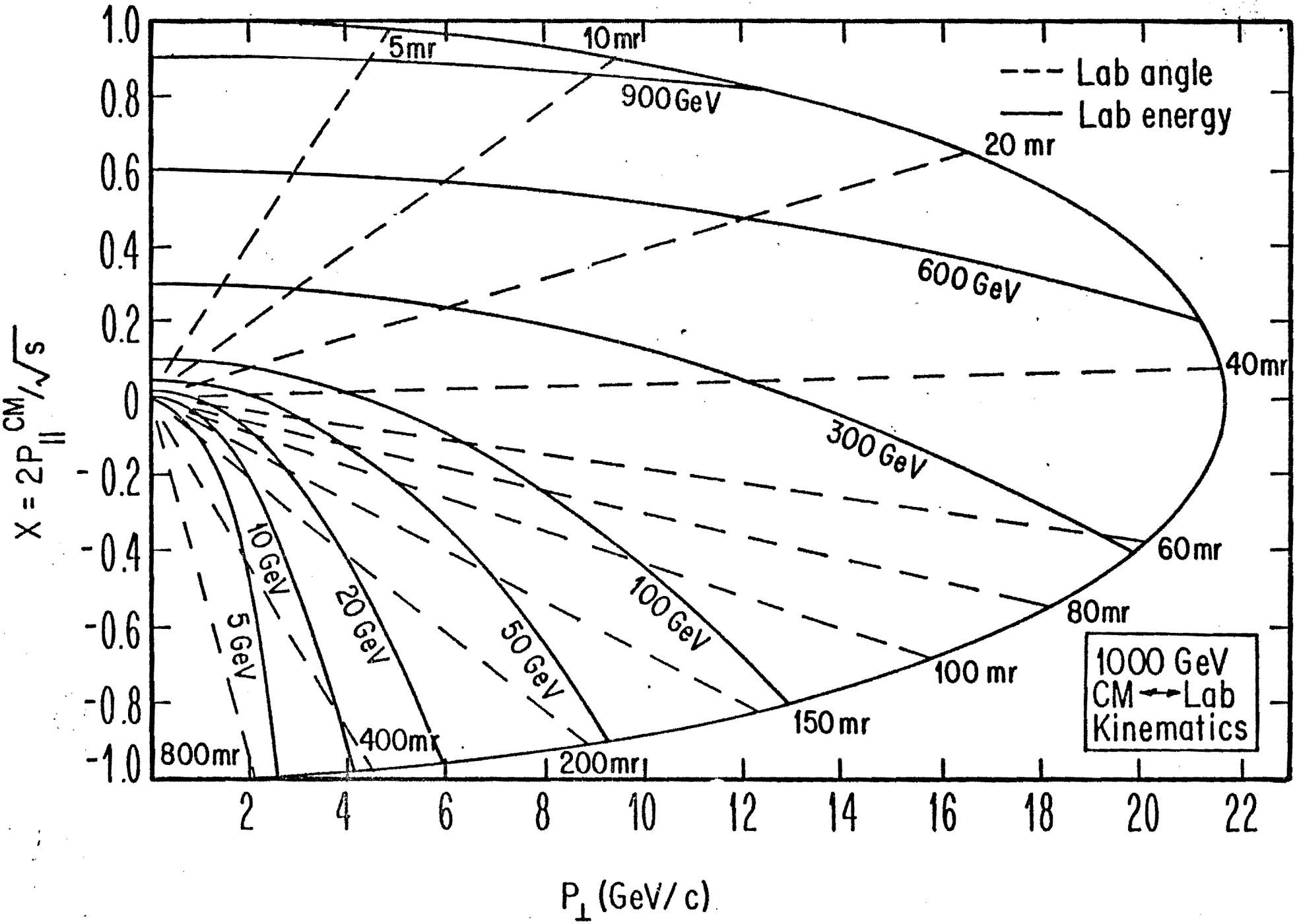
Lab angle
Lab energy
1000 GeV
CM ↔ Lab
Kinematics
5mr
10mr
20 mr
40mr
60mr
80mr
100 mr
150 mr
200mr
400mr
800mr
900 GeV
600 GeV
300 GeV
100 GeV
50 GeV
20 GeV
10 GeV
5 GeV
1.0
0.8
0.6
0.4
0.2
0
-0.2
-0.4
-0.6
-0.8
-1.0
2
4
6
8
10
12
14
16
18
20
22
$X = 2P_{\parallel}^{CM}/\sqrt{s}$
$P_{\perp}$ (GeV/c)

Fig. 26

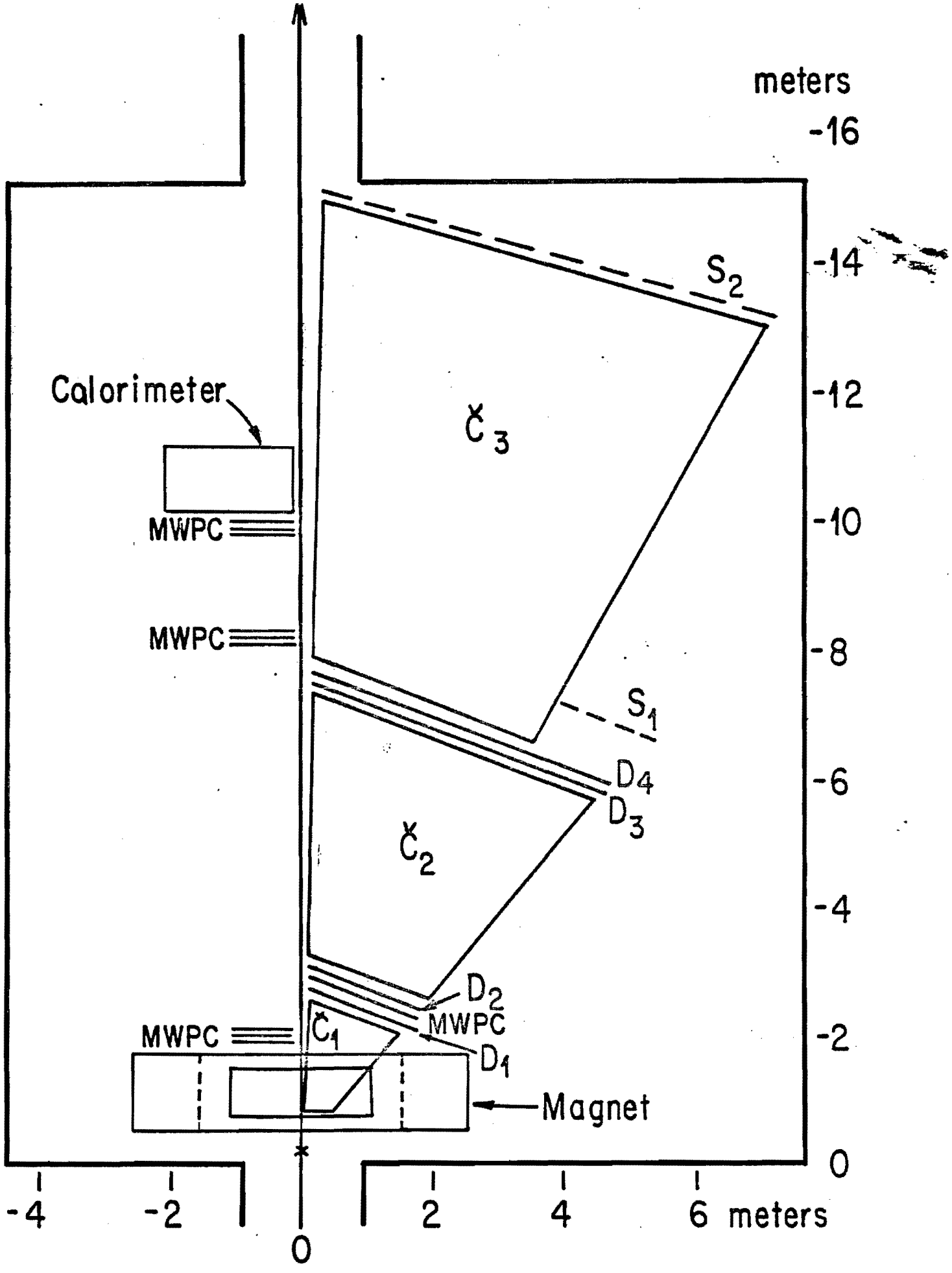
meters
-16
-14
-12
-10
-8
-6
-4
-2
0
S_2
Calorimeter
C_3
MWPC
MWPC
S_1
D_4
D_3
C_2
D_2
MWPC
MWPC
C_1
D_1
Magnet
-4
-2
0
2
4
6 meters

FIG. 3

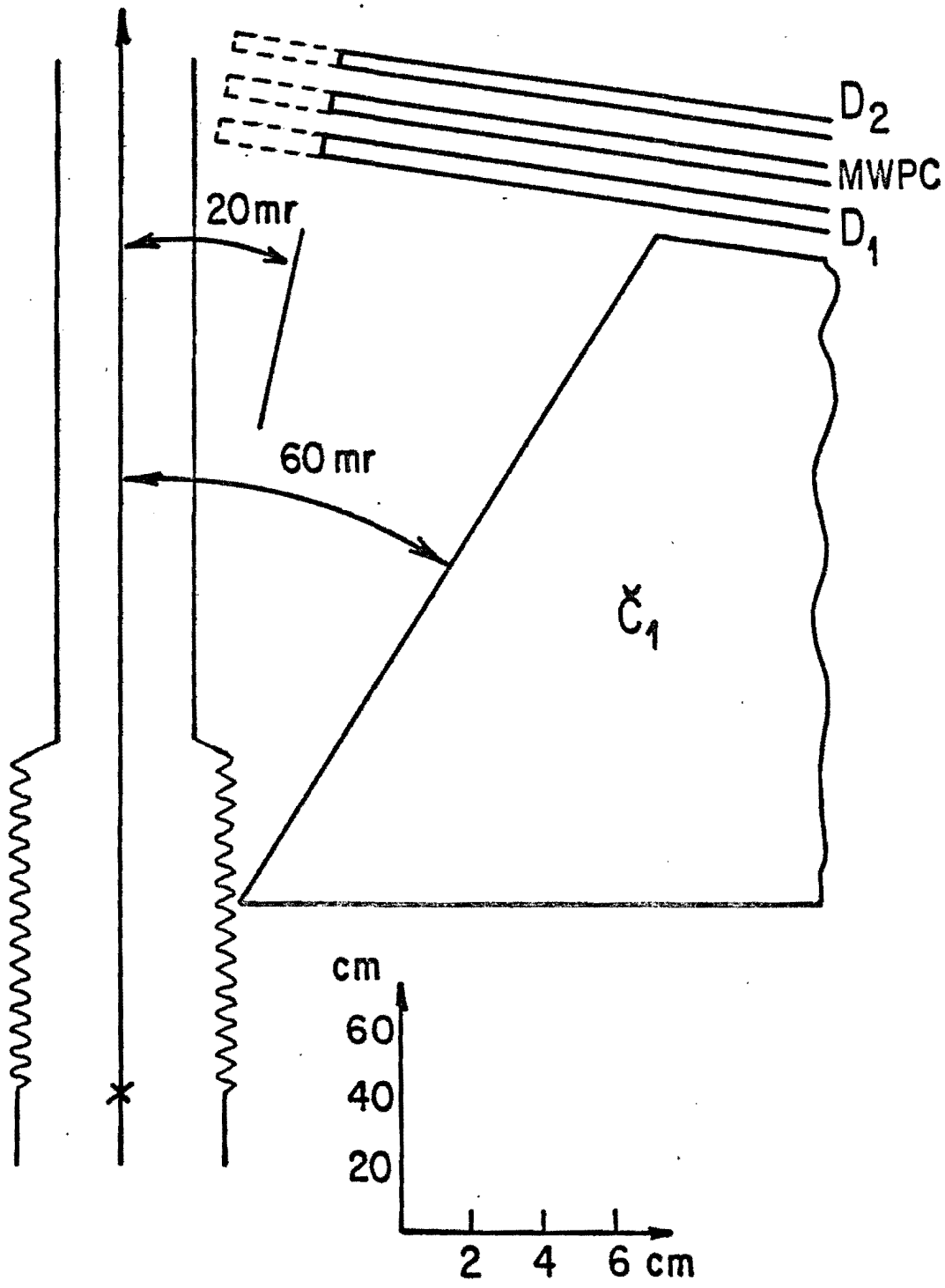
D2
MWPC
D1
20mr
60 mr
C1
cm
60
40
20
2
4
6 cm

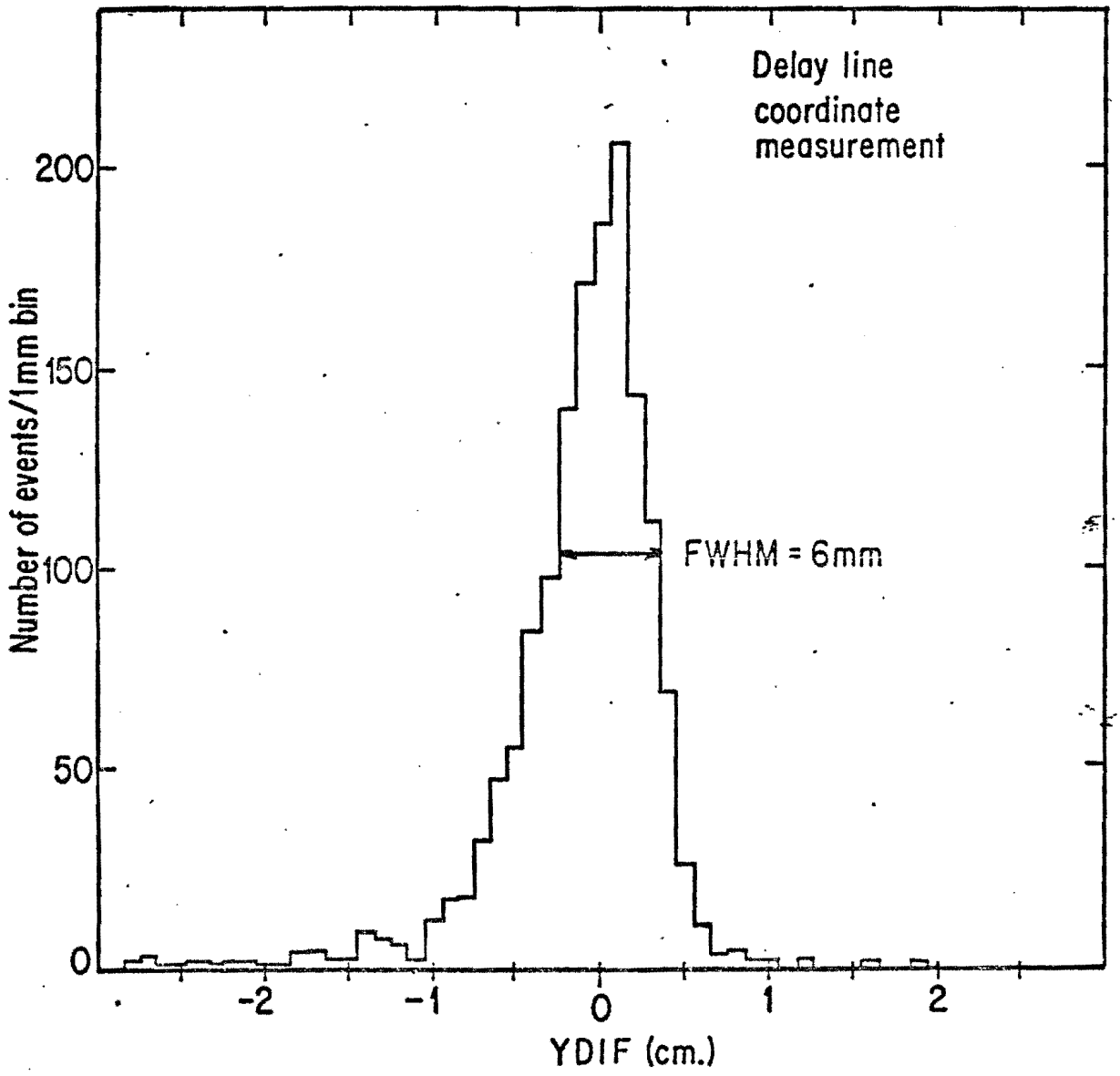
Delay line
coordinate
measurement
FWHM = 6mm
Number of events/1mm bin
200
150
100
50
0
-2
-1
0
1
2
YDIF (cm.)

FIG. 5

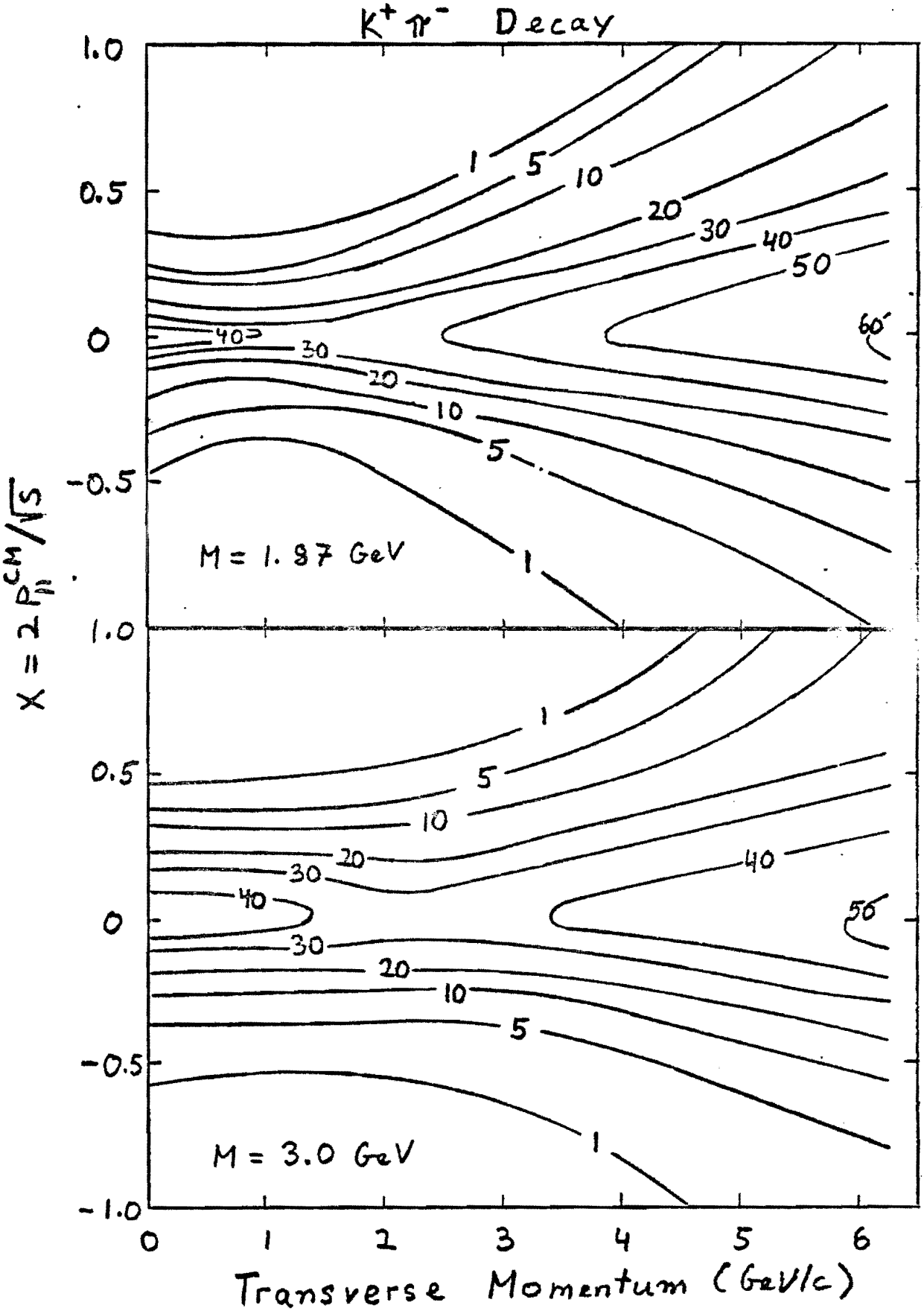
$K^+\pi^-$ Decay
1.0
0.5
0
-0.5
1.0
0.5
0
-0.5
-1.0
0
1
2
3
4
5
6
1
5
10
20
30
40
50
60
40
30
20
10
5
1
M = 1.87 GeV
1
5
10
20
30
40
50
40
30
20
10
5
1
M = 3.0 GeV
$X = 2P_{\parallel}^{CM}/\sqrt{s}$
Transverse Momentum (GeV/c)

FIG. 6

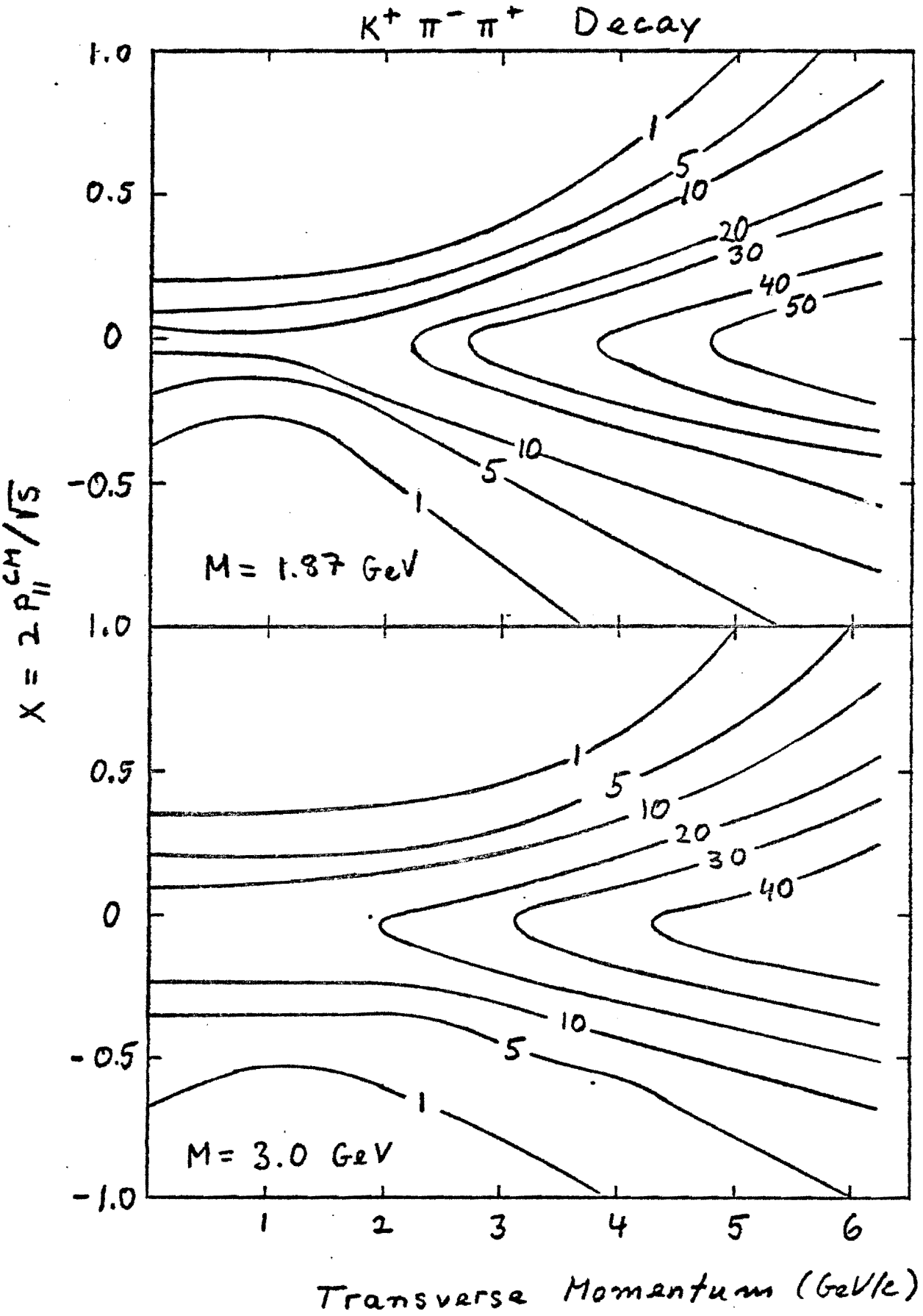
$K^+ \pi^- \pi^+$ Decay
1.0
0.5
0
-0.5
1.0
0.5
0
-0.5
-1.0
1
5
10
20
30
40
50
M = 1.87 GeV
M = 3.0 GeV
$X = 2P_{\parallel}^{CM}/\sqrt{s}$
1
2
3
4
5
6
Transverse Momentum (GeV/c)

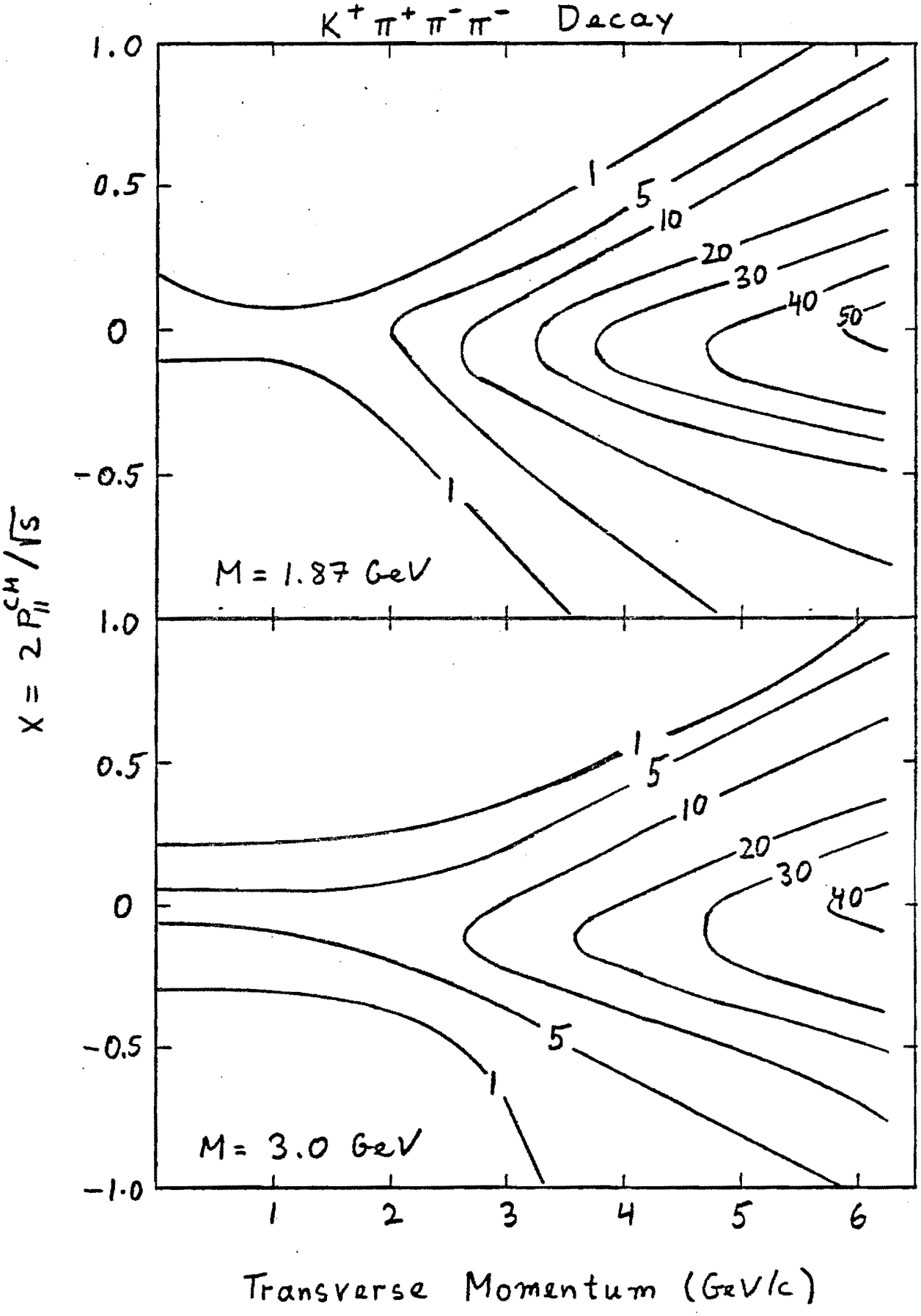
$K^+\pi^+\pi^-\pi^-$ Decay
1.0
0.5
0
-0.5
1.0
0.5
0
-0.5
-1.0
1
5
10
20
30
40
50
1
M = 1.87 GeV
1
5
10
20
30
40
5
1
M = 3.0 GeV
1
2
3
4
5
6
$X = 2P_{11}^{CM}/\sqrt{s}$
Transverse Momentum (GeV/c)

FIG. 2

400 Gev on Tungsten

Jet trigger rate per spill

assumes: (a) P-519 Geometry
(b) Cronin et al. high $P_\perp$
(c) $\frac{\text{Jet}}{\text{single particle}}$ (high $P_\perp$) = 100
(d) 10^{10} beam/spill
($\Rightarrow 5 \times 10^6$ interactions/spill)

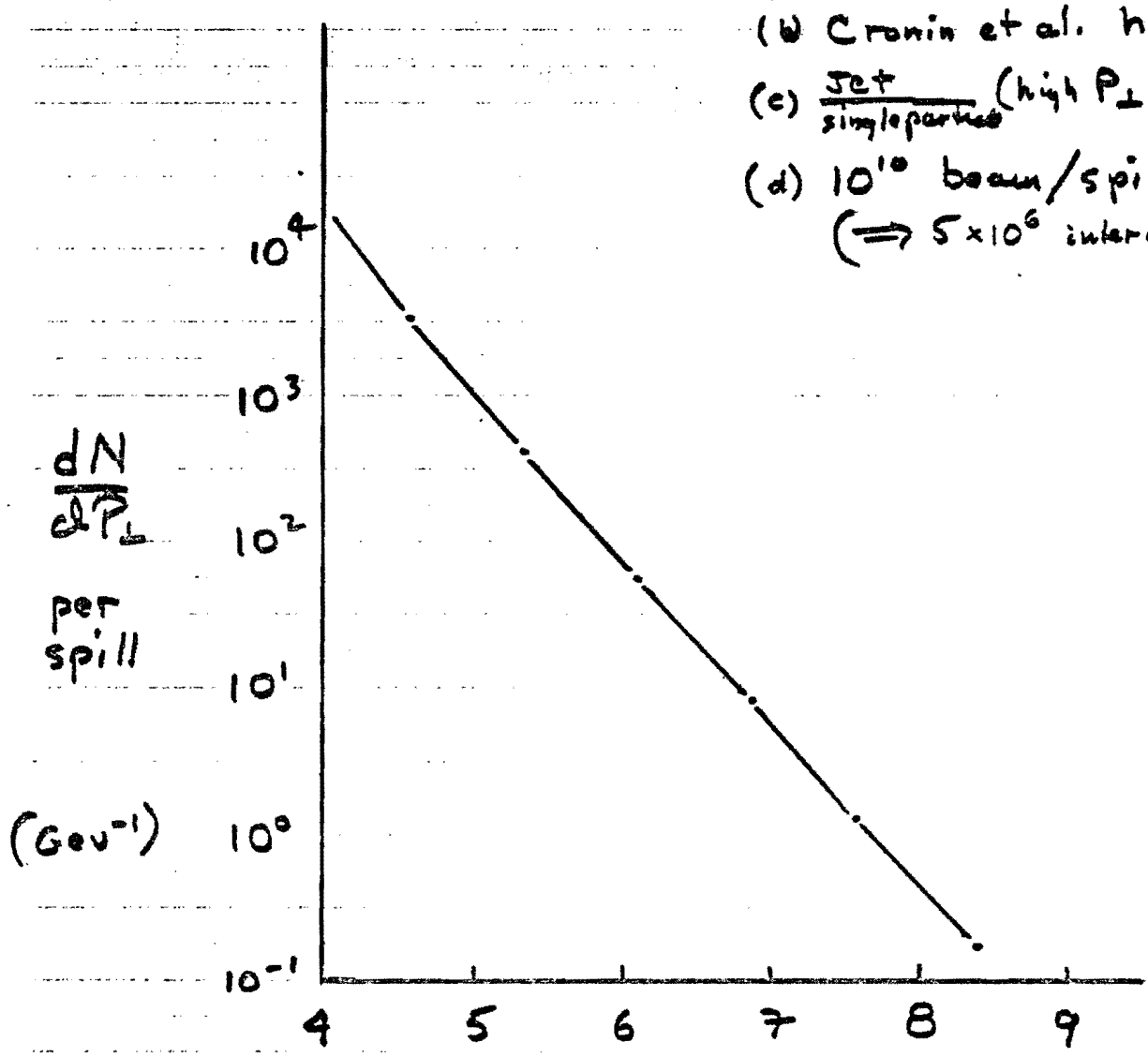

March 5, 1977

ADDENDUM TO P-519 (UCLA-VPI)

During the six months since the P-519 proposal was written, we have done additional work on improving the layout and studying its capabilities. There are several points which we would like to communicate to the PAC. These are enumerated below.

(1) Λ, $\overline{\Lambda}^{o}$, K^{o}, Ξ^{-}, Ω^{-} Detection

We pointed out in the proposal that the configuration on the west side of the beam line (chamber system packed in front of the calorimeter) allowed for a long decay path and large acceptance measurement of V^{o}'s; the V^{o}'s are reconstructed without a magnet (this capability is one of the central and key features of 519). We have since looked into these measurements in detail. Figure 1 shows the decay kinematics relationship between the pion and proton angles (measured with respect to the Λ^{o} direction) for several Λ^{o} momenta. One event corresponds to a measured point on this plane (with an accuracy of 10^{-4} radian) and leads to a determination of the Λ^{o} momentum with an uncertainty given by the curves in Figure 2. Substantially more than 50% of the decay solid angle of the Λ^{o}'s is in a kinematic region (curves well separated in Figure 1) which allows a good determination of the Λ^{o} momentum.

The physical region for K^{o} decay lies mostly outside the Λ^{o} region in Figure 1, although there is some overlap. K^{o} background inside the Λ^{o} region is easily corrected for statistically from measurement of the K^{o}'s outside the Λ^{o} region. To aid in this separation on an event-by-event basis without sacrificing decay volume and to have the option to use Cerenkov logic in the trigger as mentioned below, we will construct a relatively small Cerenkov counter C_4 to be positioned as shown in Figure 1 with cells that match the calorimeter modules. A low magnetic field ($\sim$ 200 Gauss) Helmholz coil in this region will permit charge identification and separation of Λ^{o} from $\overline{\Lambda}^{o}$.

Finally, we remark that the Λ^{o} measurement capability allows the easy identification of $\Xi^{-} \rightarrow \Lambda^{o}\pi^{-}$ and $\Omega^{-} \rightarrow \Lambda^{o}K^{-}$. For example, Figure 3 shows the signal obtained in the recent UCLA-Saclay ISR experiment R603. The measured Ξ^{-} cross section implies that about 10^{-2} of all Λ^{o} come from Ξ decay. (Λ^{o} are produced in $\sim$8% of all interactions at high energies.) The trigger efficiency for Λ^{o}'s can be greatly enhanced by performing hardware logic on the chamber signals before the calorimeter and by matching cells of C_4 with calorimeter cells to select fast protons. A higher level of logic can also be used to trigger on Ξ^{-} and Ω^{-}. The expected number of high P_t Λ^{o} and

$\bar{\Lambda}^o$ recorded per 100 hours (with the use of the calorimeter trigger) is shown in Figure 4. The assumptions used in these estimates are shown on the Figure. Note that these are just the Λ^o's triggered on by virtue of their high P_t detected in the calorimeter. Λ^o's pointing into any other part of the spectrometer aperture will also be detected but will tend not to have as high P_t. All of these strange particles will be used in invariant mass combinations with other tracks in our search for new charmed states. In particular, any observed longitudinal polarization of Λ^o (not coming from Ξ) or of Ξ^- would be positive proof of their new weak interaction origin (even without the detection of other tracks).

(2) Evidence for Charmed Particle Production in Hadronic Interactions

Figure 5 shows the $\Lambda^o\pi^+\pi^+\pi^-$ mass spectrum observed by the UCLA-Saclay ISR collaboration. The enhancement at 2260 MeV appears to be the charge conjugate state of the one observed at Fermilab. The observed width of 44 MeV (less than the 80 MeV bin widths shown in Figure 5) agrees with the calculated resolution (σ = 21 MeV) of the apparatus. The curve shows the calculated acceptance of the apparatus. The observed $B\cdot\sigma$ = 0.4 μbarn for the 2260 signal in the region $x > 0.7$. It should be noted that, although x is large, this is not diffractive excitation because the charge multiplicity of these events is quite large.

In general, experience seems to be that resonance observation at large x is easier than at small x because of the relative suppression of combinatorial background involving central region pions. Near x = 0 but at larger P_t, combinatorial background should be reduced for the same reasons. Thus, for example, a clear ρ^o signal appears in an E-260 di-pion mass spectrum only at larger P_t ($\sim$ 3 GeV/c). This is related to the fact that for production of particles or systems of particles with $P_t \lesssim 3$ GeV/c, there is a clear correlation between mass and slope of P_t dependence; the slopes become flatter with increasing mass.

It may be argued that the observation of the $\Lambda 3\pi$ state at 2260 MeV implies that a large x, low P_t experiment is the one to do. We think not, however. 90^o CM high P_t experiments are much more advantageous in that: (1) they are easier to trigger on, (2) low momentum particles are more easily measured, (3) Cerenkov identification is manageable. P-519 will be a powerful instrument for probing high energy hadronic interactions at Fermilab. The experiment maximizes: rate, acceptance, high-P_t trigger efficiency, pattern recognition ease and most importantly, the ability to trigger and

observe high P_t, Λ^o, Ξ^- and Ω^-.

(3) Layout and Equipment

Figure 6 shows our revised layout. The apparatus is now left-right symmetric through C_2 and the chambers following it. Since we have the detailed engineering drawings for C_2, its duplication is a straight forward task with the bulk of the work farmed out (total cost of counter is less than \$60K). The acceptance for identified multi-particle states is markedly improved over that shown in the proposal. See, for example, Figure 7.

As shown below, the vacuum chamber immediately following the target consists of a 2.5 m length of CERN-ISR corregated stainless steel pipe (0.15 mm thick with 15 cm diameter) welded at a transition junction to a 12 m long conical pipe with half-angle of 10 mrad and smallest diameter of 2 inches.

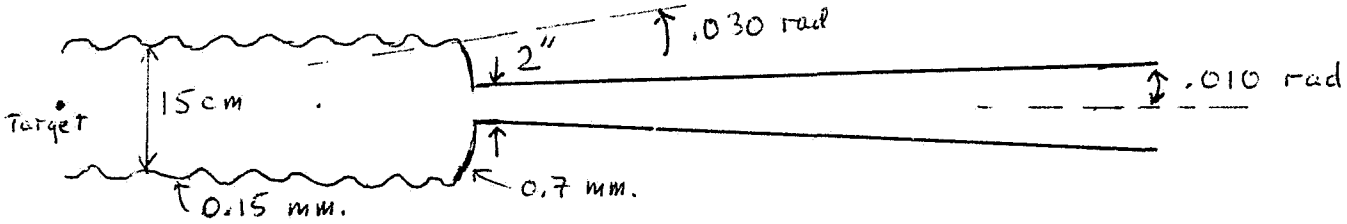

This arrangement minimizes the interaction probability of final-state particles leaving the vacuum pipe and is essential to remove event-associated "splashes" as a source of background.

We have considered the introduction of shower counters for π^o detection in the east spectrometer but do not think it essential for the first round experiment. We shall keep it as an option for a later proposal.

We remarked in the proposal that the spectrometer could be moved downstream to the pion-lab for a later experiment. It has since been suggested that an upstream target might be introduced and the beam tuned for negative particles in our present proposed location. We have not yet explored this possibility with the proton department. Coupled with the clear physics advantage of this arrangement is the obvious disadvantage that we would no longer be a transmission experiment as far as the pion-lab is concerned. It should be further remarked that we have the intention of running with a wide range of target materials to study the A-dependence of any effects we find.

Six full-time people are already working on construction of the new apparatus at UCLA and VPI. This number will grow larger over the next 6 months. In this connection, it is significant to note that E-253 is now

completely installed, thus freeing Luke Mo and his group considerably. Moreover, Tom Nunamaker is now employed one-half time by VPI at Fermilab and can start working immediately on the electronics for 519.

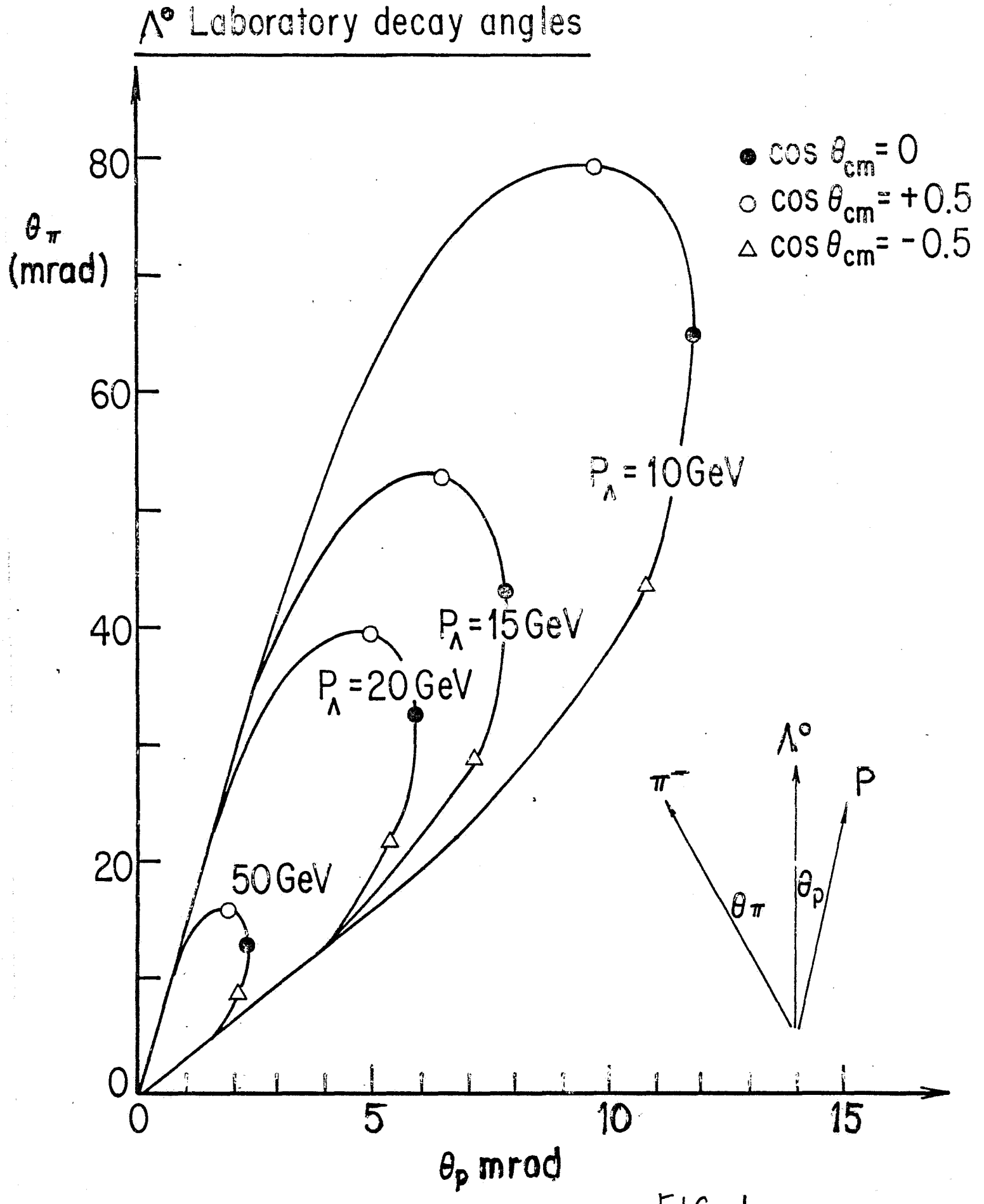
Λ° Laboratory decay angles
● cos θcm = 0
○ cos θcm = +0.5
△ cos θcm = -0.5
θπ (mrad)
80
60
40
20
0
PΛ = 10 GeV
PΛ = 15 GeV
PΛ = 20 GeV
50 GeV
Λ°
π⁻
P
θπ
θp
0
5
10
15
θp mrad

FIG. 1

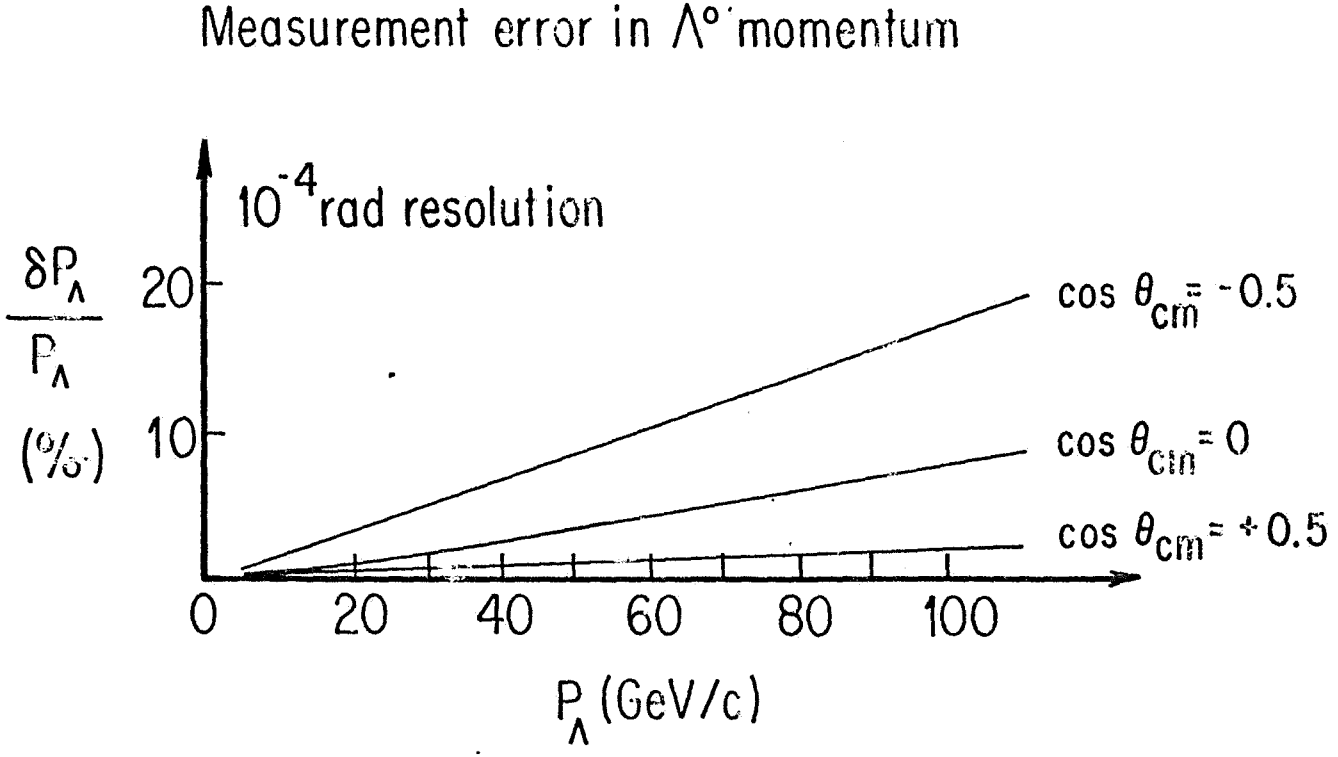
Measurement error in Λ° momentum
10^{-4} rad resolution
$\frac{\delta P_\Lambda}{P_\Lambda}$ (%)
20
10
0
20
40
60
80
100
P_Λ (GeV/c)
cos θ_{cm} = -0.5
cos θ_{cm} = 0
cos θ_{cm} = +0.5

FIG. 2

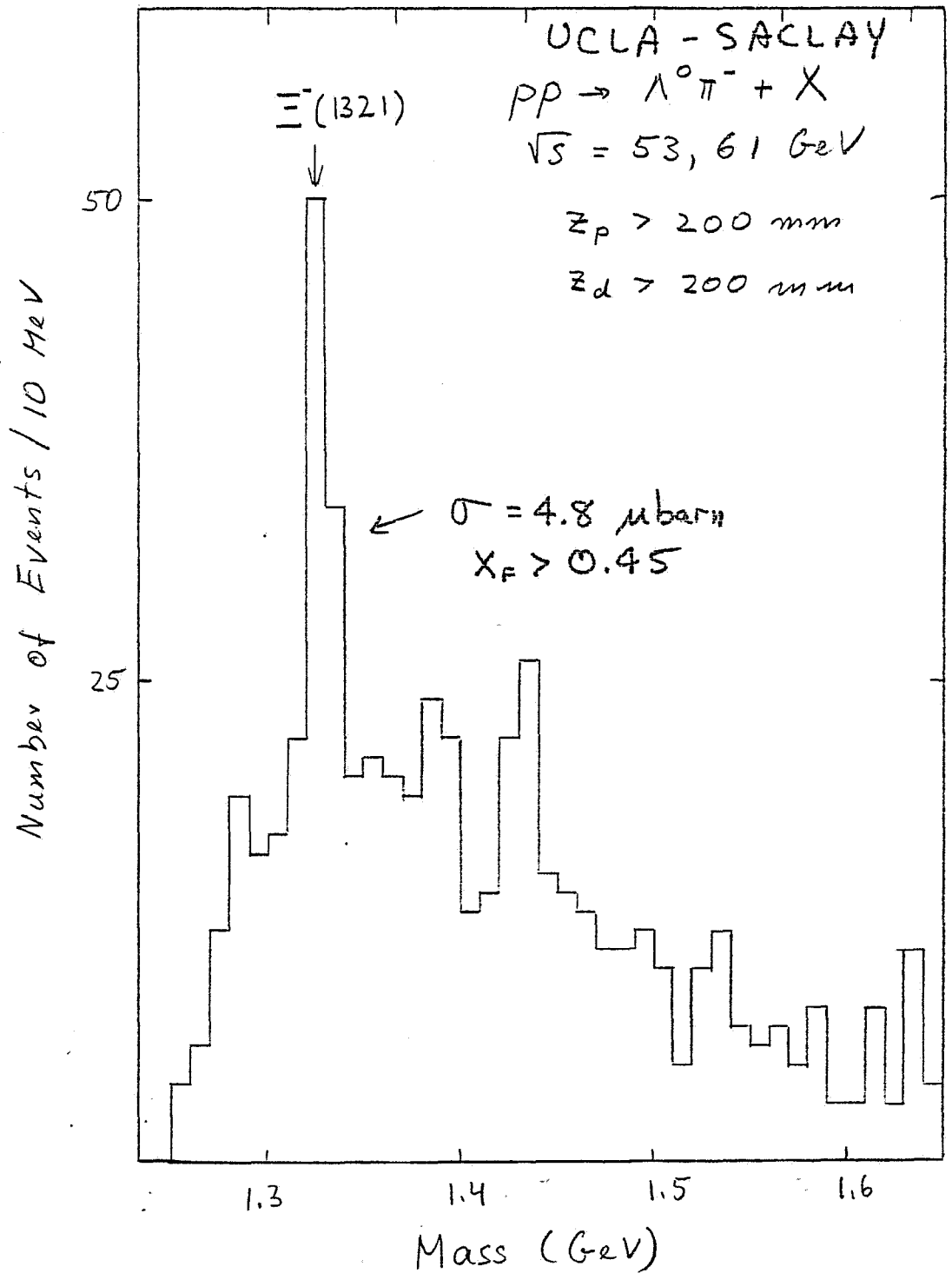
UCLA - SACLAY
$pp \to \Lambda^0 \pi^- + X$
$\sqrt{s}$ = 53, 61 GeV
$z_p > 200$ mm
$z_d > 200$ mm
$\Xi^-(1321)$
$\sigma = 4.8$ μbarn
$x_F > 0.45$
Number of Events / 10 MeV
50
25
1.3
1.4
1.5
1.6
Mass (GeV)

FIG. 3

Number of recorded Λ° per 100 hours per GeV P_t

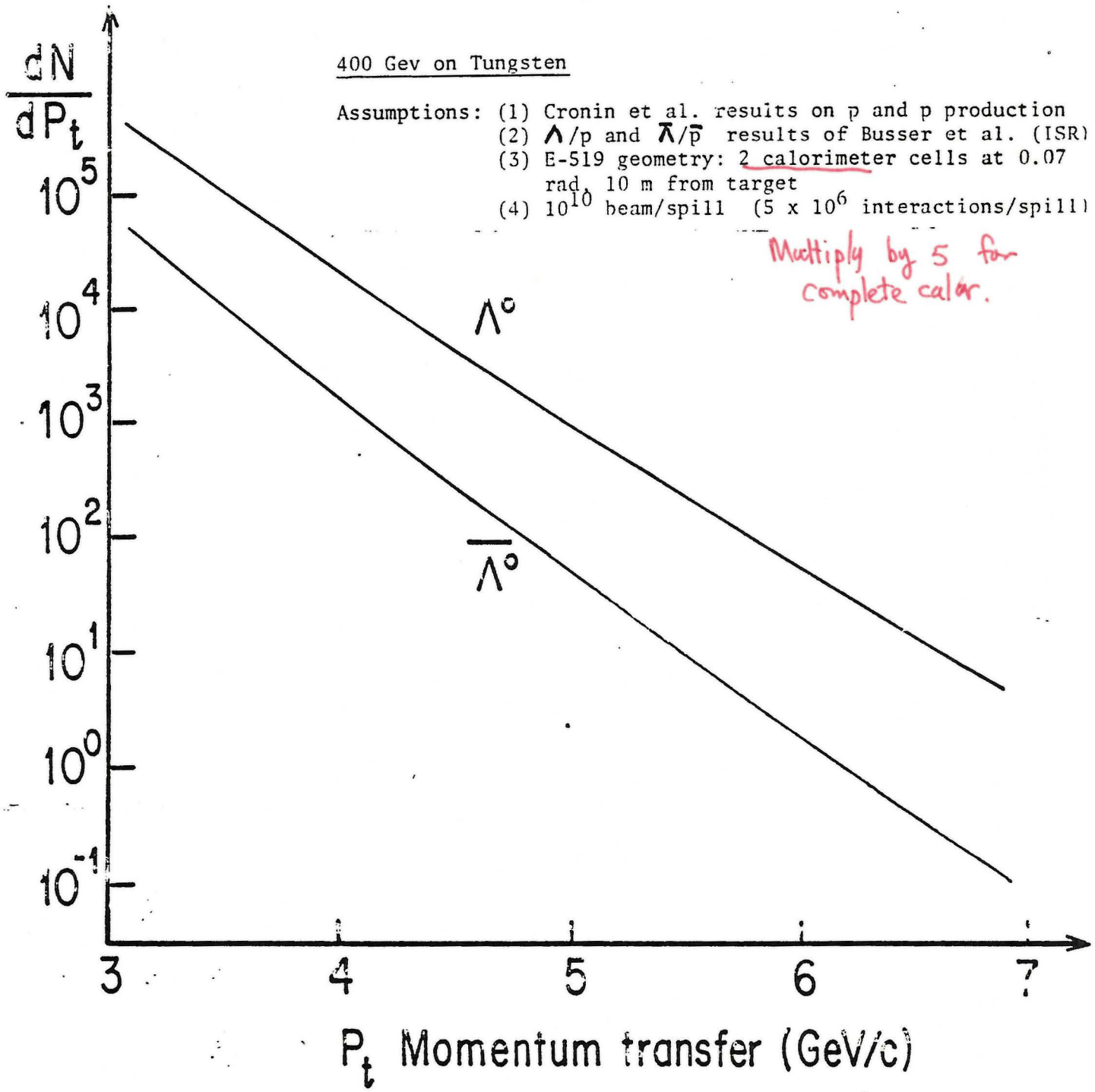

FIG. 4

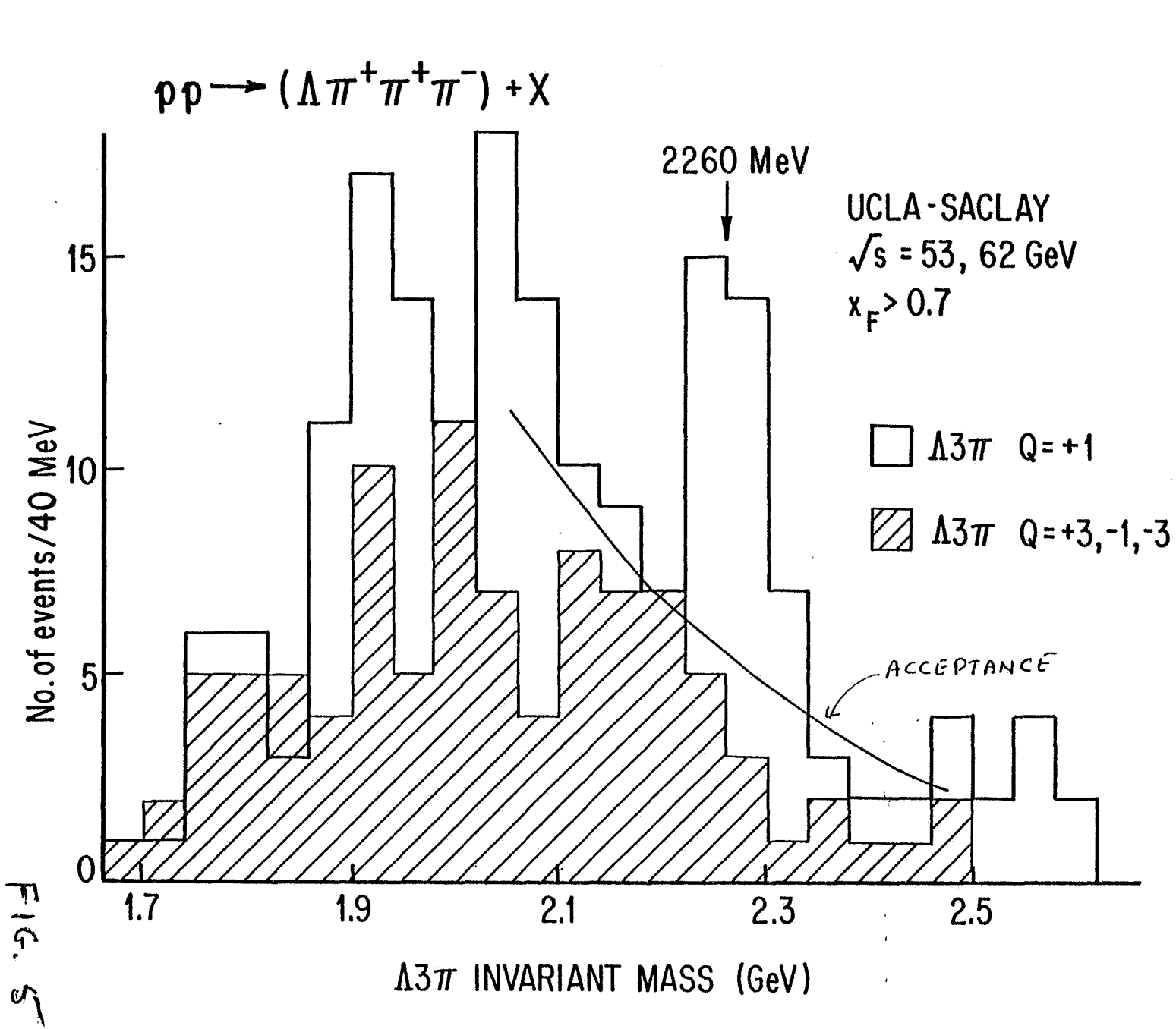
$pp \rightarrow (\Lambda\pi^+\pi^+\pi^-) + X$
2260 MeV
UCLA-SACLAY
$\sqrt{s}$ = 53, 62 GeV
$x_F > 0.7$
$\Lambda 3\pi$ Q = +1
$\Lambda 3\pi$ Q = +3, -1, -3
ACCEPTANCE
No. of events/40 MeV
0
5
10
15
1.7
1.9
2.1
2.3
2.5
$\Lambda 3\pi$ INVARIANT MASS (GeV)

Fig. 5

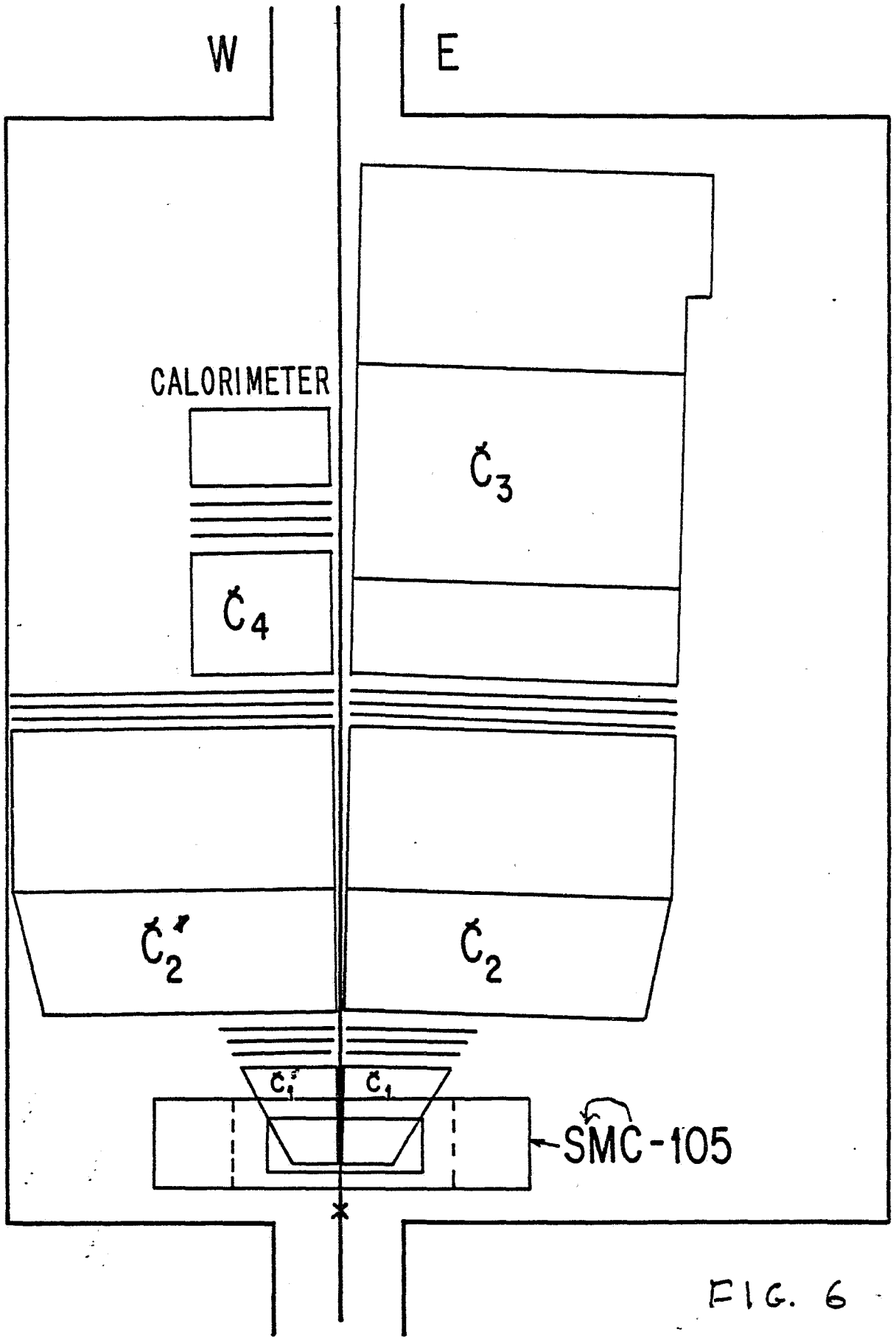
W
E
CALORIMETER
$\check{C}_3$
$\check{C}_4$
$\check{C}_2'$
$\check{C}_2$
$\check{C}_1'$
$\check{C}_1$
SMC-105

FIG. 6

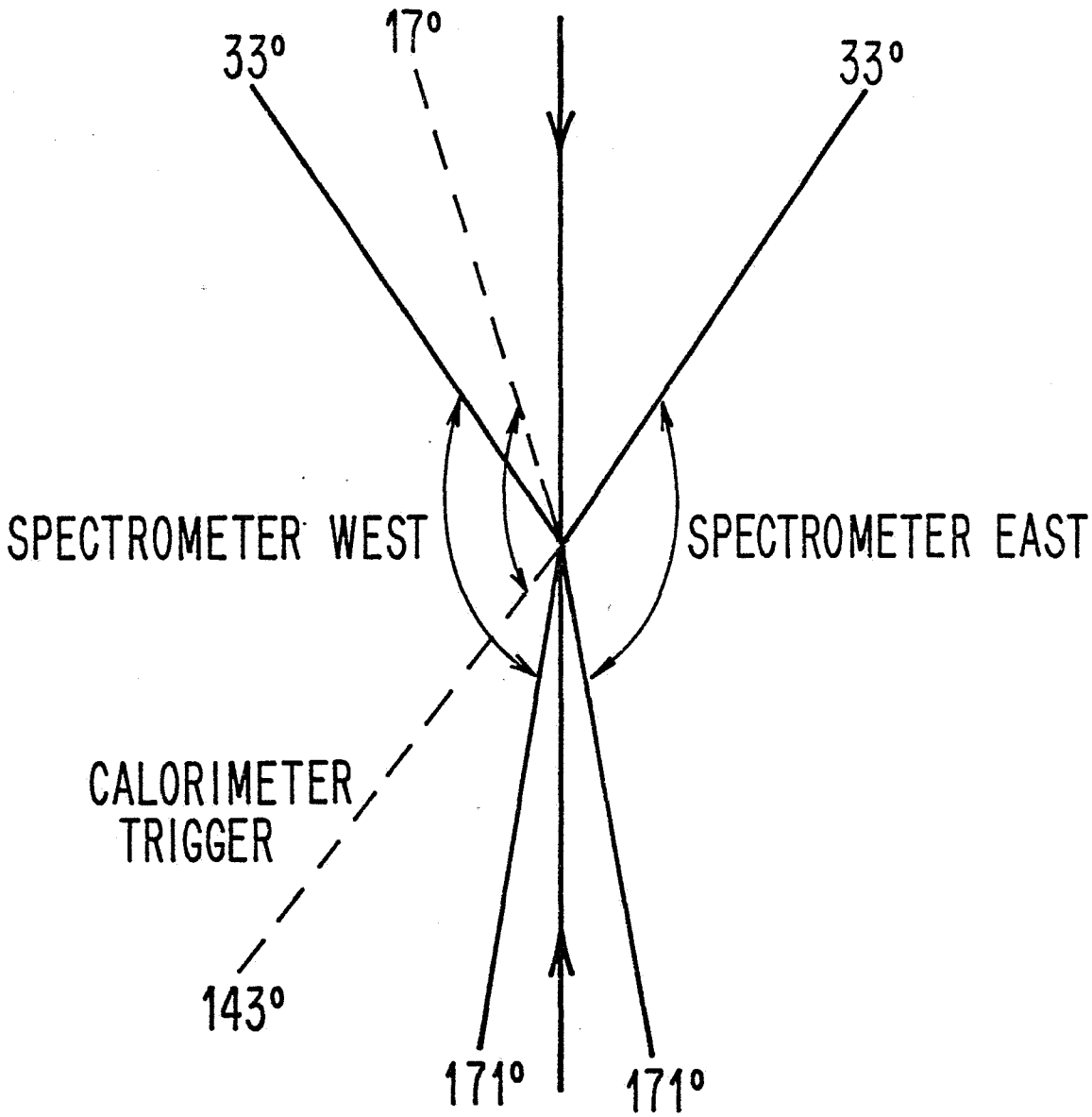
33°
17°
33°
SPECTROMETER WEST
SPECTROMETER EAST
CALORIMETER
TRIGGER
143°
171°
171°

FIG. 7